Multiobjective Optimization of ESG Bond Portfolios: A Copula-Based Dynamic Nelson-Siegel Approach*

Maziar Sahamkhadam & Andreas Stephan†

February 3, 2025

Abstract

This paper presents a copula-based pricing framework for forecasting bond returns and optimizing multi-objective bond portfolios (MOBPs). Utilizing a copula-based dynamic factor model, we generate step-ahead forecasts for zero-coupon bond yields, which are subsequently applied to price both callable and non-callable fixed-coupon bonds. These simulated bond prices serve as inputs for convex multi-objective portfolio optimization, incorporating key criteria such as average returns, Conditional Value-at-Risk (CVaR), distance-to-default, transaction costs, and option-adjusted duration and convexity. Applying our methodology to a dataset of 879 ESG bonds denominated in Euros from January 2016 to July 2024, we demonstrate that the proposed MOBP approach consistently outperforms an equally weighted benchmark in terms of higher returns and Sharpe ratios while effectively mitigating tail risk. Notably, our framework enhances portfolio resilience during periods of market turbulence, such as the COVID-19 pandemic and the Russo-Ukrainian war, underscoring its applicability in risk-sensitive sustainable investing.

JEL: G11, G23, G30, D62

Keywords: Bonds, ESG, portfolio optimization, vine copula, dynamic factor model

*Financial support for this project through a Nasdaq Nordic Foundation grant is gratefully acknowledged. The contents of this paper are solely the responsibility of the authors and do not reflect the views of the Nasdaq Nordic Foundation. We also thank participants at the Computational Financial Econometrics conference 2024 in London for helpful comments and suggestions. The usual disclaimer applies.

†Linnaeus University, School of Business & Faculty of Technology
Corresponding author: Maziar Sahamkhadam, Maziar.Sahamkhadam@lnu.se

1 Introduction

Environmental, Social, and Governance (ESG) bonds have emerged as a significant asset class in modern bond portfolio management. By emphasizing sustainable investment, ESG bonds enable investors to align their financial objectives with environmental responsibility, social equity, and ethical governance. The rising demand for sustainable investing is driven by increasing investor awareness and evolving regulatory requirements. According to the Global Sustainable Investment Alliance (GSIA), sustainable investments reached $30.3 trillion worldwide in 2022, reflecting a 20% increase in non-U.S. markets—including Europe, Canada, Japan, Australia, and New Zealand-compared to 2020 (GISA, 2022). Additionally, the Climate Bond Initiative (CBI) reported that $5.5 trillion was invested in green, social, sustainability, and sustainability-linked bonds in 2023, with $4.4 trillion aligning with CBI standards (CBI, 2023). These figures underscore the rapid expansion of sustainable fixed-income investments, reinforcing their role in the evolving financial landscape.

This study contributes to the existing literature by introducing a copula-based dynamic Nelson-Siegel framework for modeling the term structure of interest rates, incorporating tail dependence to enhance yield curve forecasting. Additionally, it extends multiobjective bond portfolio optimization by integrating ESG considerations, credit risk, and duration-convexity trade-offs, providing a robust methodology for risk-adjusted bond portfolio management during periods of market stress.

There are two main general approaches to the optimization of bond portfolios. The first is to obtain the optimal weights based on the cash flows generated from the fixed-income assets (see e.g., Bradley and Crane, 1972; Hodges and Schaefer, 1977; Ronn, 1987; Zenios, 1995). The second approach is to estimate the expected returns and volatility of the bond portfolio, e.g., by using a factor model of the term structure, and to obtain the optimal weights based on Markowitz's mean-variance framework (see, e.g., Zumbach, 2013; Caldeira, Moura and Santos, 2016, 2018). In addition, only a handful of existing studies on bond portfolio optimization include coupon-paying bonds (Deguest, Fabozzi, Martellini and Milhau, 2018), callable bonds (Vassiadou-Zeniou and Zenios, 1996), and utilize tail risk as the portfolio risk measure (Tu and Chen, 2018).

To model zero-coupon bond yields, known as the yield curve or interest rate term structure, many studies, e.g., Vasicek (1977), Cox, Ingersoll Jr and Ross (1985), Duffie and Kan (1996), Dai and Singleton (2000), suggest affine arbitrage-free term structure models. These models typically consider unobserved factors that can be utilized to explain the entire set of yields. Duffee (2002) show that these standard models provide poor forecasts for Treasury yields. Nelson and Siegel (1987) suggest an alternative approach with a three-dimensional parameter that parsimoniously models the entire yield curve. Based on Nelson and Siegel (1987)'s exponential components framework, Diebold and Li (2006) suggest the dynamic Nelson-Siegel model and show that

the three time-varying factors can be interpreted as level, slope, and curvature. Indeed, the dynamic Nelson-Siegel model is a statistical three-factor model. Diebold, Rudebusch and Aruoba (2006) show that the dynamic Nelson-Siegel model can be presented as a state space model. Other extensions to the dynamic Nelson-Siegel model include allowing for macroeconomic non-latent factors (Diebold et al., 2006; Levant and Ma, 2016), time-varying parameters (Koopman, Mallee and Van der Wel, 2010; Byrne, Cao and Korobilis, 2017), arbitrage-free restrictions (Christensen, Diebold and Rudebusch, 2009, 2011). Although term structure modeling is a well-established area in fixed-income research, the (tail) dependence structure among zero-coupon yields (interest rates) has been ignored when pricing coupon-paying bonds.

In this paper, we propose a copula-based approach to term structure modeling, integrating the parsimonious dynamic Nelson-Siegel model to generate point forecasts for governmental zero-coupon yields. To capture dependencies between these yields, we employ a Regular vine (R-vine) copula model, enabling the simulation of step-ahead conditional distributions for the yield curve. Building on the coupon-bond pricing framework of Deguest et al. (2018) and extending it to callable bonds as in Dunetz and Mahoney (1988), we derive step-ahead simulations for bond returns. Furthermore, we develop a multiobjective bond portfolio optimization system that incorporates multiple criteria, including average return, Conditional Value-at-Risk (CVaR), ESG score, distance-to-default (as a credit risk measure), turnover, and (option-adjusted) duration and convexity. The resulting scenario-based multiobjective optimization problem is solved using the weighted-sum approach and linear programming.

Using a sample of 19 German governmental zero-coupon daily yields as a proxy for the EU yield curve, our analysis reveals that (i) the assumption of uncorrelated deviations from the yield curve holds only for zero-coupon yields with significantly different maturities, and (ii) tail dependence exists among near-term yields, supporting the use of symmetric and asymmetric tail dependence models in interest rate forecasting.

Drawing on a dataset of 879 ESG bonds traded in Euro currency from 2016 to 2024, we construct multiobjective bond portfolios (MOBPs) employing a rolling window approach and assess their performance against an equally weighted benchmark. Our findings demonstrate that the proposed copula-based dynamic Nelson-Siegel model and MOBP methodology enhance portfolio risk mitigation and improve risk-adjusted returns during market downturns, such as the COVID-19 pandemic and the Russo-Ukrainian war.

The current study contributes to the field of bond valuation and portfolio optimization in several aspects. First, we extend the classical dynamic Nelson-Siegel model and incorporate non-parametric dependency structure between governmental zero-coupon yields. In doing so, we propose a forecasting approach that applies the dynamic latent factor model suggested in Diebold et al. (2006) and the R-vine copula model. This approach is different from those suggested previously, for example in Junker, Szimayer and Wagner (2006), where the copulas are applied to

model the nonlinear dependence between latent factors deriving the term structure. Instead, we model the tail dependency between the yields directly and obtain a joint distribution from the marginal distributions estimated using the dynamic yield curve model. Second, we extend the no-arbitrage coupon-bond pricing model in Deguest et al. (2018) to incorporate (i) the suggested copula-based dynamic Nelson-Siegel zero-coupon bonds, and (ii) callable bond prices, duration, as well as, convexity based on the pricing model suggested in Dunetz and Mahoney (1988). Finally, we develop a multiobjective convex portfolio system that incorporates several portfolio attributes related to bond investment, namely, bond portfolio expected return, conditional Value-at-Risk (CVaR), duration, convexity, distance-to-default, turnover, as well as, issuers' corporate social responsibility measured as ESG scores.

The remainder of this paper is structured as follows: Section 2 presents the methodology, including vine copulas, term structure models, coupon-paying bond pricing, multiobjective optimization, as well as the steps involved in constructing the copula-based MOBPs. Section 3 presents the data. We provide our empirical analysis in Section 4. Finally, concluding remarks are presented in Section 5.

2 Methodology

2.1 Vine Copulas

According to Sklar's theorem, any multivariate cumulative distribution function F for a random variable set $(Z_1, ..., Z_N)$ consists of a N-dimensional copula C and marginal distributions $F_1, ..., F_N$, such that

$$\forall \mathbf{z} \in \Re^N : F(z_1, z_2, \ldots, z_d) = C(F_1(z_1), F_2(z_2), \ldots, F_N(z_N)) = C(u_1, u_2, \ldots, u_N), \quad (1)$$

where $z_i = F_i^{-1}(u_i)$, $u_i \sim U[0,1]^N, \forall i \in \{1, 2, \ldots, N\}$. Assuming all the marginal distribution functions are continuous, then C is unique and defined as the joint distribution of $(U_1, ..., U_N) = (F_1(Z_1), ..., F_d(Z_N))$. Let $\mathbf{\Omega}$ be a set of parameters of the copula function $C(u_1, u_2, \ldots, u_N|\mathbf{\Omega})$ and f_i be the derivative of the univariate marginal distribution F_i. We can write the density function for the N-dimensional multivariate distribution as

$$\begin{aligned} f(z_1, z_2, \ldots, z_N) &= \frac{\partial^N C(F_1(z_1), F_2(z_2), \ldots, F_N(z_N)|\mathbf{\Omega})}{\partial z_1, \partial z_2, \ldots, \partial z_N} \\ &= c(F_1(z_1), F_2(z_2), \ldots, F_N(z_N)|\mathbf{\Omega}) \times \prod_{i=1}^{N} f_i(z_i), \end{aligned} \quad (2)$$

where c is the copula density function, with log-likelihood function

$$\mathcal{L}((z_1, z_2, ..., z_N)|\mathbf{\Omega}) = \sum_{t=1}^{T} \left[\sum_{i=1}^{N} \log f_i(z_{ti}) + \log\left[c(u_{t1}, u_{t2}, ..., u_{tN}|\mathbf{\Omega})\right] \right]. \quad (3)$$

Note that in Eqs. (1)–(2), only one copula function C is used to construct the joint distribution, which means only one copula family is used for the entire set of marginal uniforms $u_1, u_2, \ldots, u_N$. While Joe (1996) suggests a decomposition of c into products of pair-wise densities, Bedford and Cooke (2001, 2002) derive a graphical representation, called a regular vine (Rvine), of the pair-copula construction in the form of nested trees. Aas, Czado, Frigessi and Bakken (2009) develop maximum likelihood inference and estimation of three vine models with arbitrary pair-copulas (including Archimedean families). More properties and statistical inference for vine copulas have been developed by Joe (2014) and Czado (2019).

For a N-dimensional set of continuous random variables, there exist $N(N-1)/2$ pair-copulas, and the copula density c can be decomposed into a product of these pair-copulas' densities. Using a sequence of $h = 1, 2, \ldots, N-1$ linked trees, the decomposition can be presented in a graphical PCC, known as the regular vine. Let $e \in E_h$ be the edge between two nodes n_e, k_e, representing a pair-copula $c_{n_e,k_e;D_e}$ conditioned on D_e, with copula parameter(s) $\mathbf{\Omega}_{n_e,k_e|D_e}$. Let $\boldsymbol{u}_{D_e} = \{u_i|h \in D_e\}$ be the variables in the conditioning set D_e. Let $C_{n_e|D_e}$ be the conditional

distribution of $U_{ne}|\boldsymbol{U}_{D_e}$. When the number of trees increases, the conditioning set D_e also grows, and it is common to consider only the dependence of $c_{n_e,k_e;D_e}$ on the indexes in D_e, ignoring the impact of $\boldsymbol{u}_{D_e}$. This is the so-called simplifying assumption (see Acar, Genest and NešLehová, 2012; Haff et al., 2013). The copula density for a simplified Rvine copula is

$$c\left(u|\boldsymbol{\Omega}\right)=\prod_{h=1}^{N-1}\prod_{e\in E_h}c_{n_e,k_e;D_e}\left(C_{n_e|D_e}(u_{n_e}|\boldsymbol{u}_{D_e}),C_{k_e|D_e}(u_{k_e}|\boldsymbol{u}_{D_e})|\boldsymbol{\Omega}_{n_e,k_e|D_e}\right), \tag{4}$$

with log-likelihood function

$$\mathcal{L}(\boldsymbol{\Omega}|u)=\sum_{i=1}^{N}\sum_{h=1}^{N-1}\sum_{e\in E_i}\ln\left[c_{n_e,k_e;D_e}\left(C_{n_e|D_e}(u_{i,n_e}|u_{i,D_e}),C_{k_e|D_e}(u_{j,k_e}|u_{j,D_e})|\boldsymbol{\Omega}_{n_e,k_e|D_e}\right)\right]. \tag{5}$$

Although vine copulas are flexible in estimating tail dependency, there is a trade-off between higher flexibility and an increased computational load in high-dimensional settings. Therefore, truncated and simplified vine structures that allow for high-dimensional dependence estimation have been developed (see e.g., Heinen, Valdesogo et al., 2009; Kurowicka, 2011; Brechmann, Czado and Aas, 2012; Brechmann and Joe, 2015). In particular, Brechmann et al. (2012) show how to truncate or simplify the Rvine structure. This truncation is applied to the number of trees in the vine by setting an independence copula at each edge from a specific tree $I\in\{1,2,\ldots,N-1\}$ to the final tree. The I-level truncated Rvine has the density

$$c^{Truncated}\left(u\right)=\prod_{h=1}^{I}\prod_{e\in E_h}c_{n_e,k_e|D_e}\left(C_{n_e|D_e}\left(u_{n_e}|u_{D_e}\right),C_{k_e|D_e}\left(u_{k_e}|u_{D_e}\right)|\boldsymbol{\Omega}_{n_e,k_e|D_e}\right). \tag{6}$$

2.2 Dynamic Factor Models for Term Structure

Let $y_t(\mathcal{T}_i)$ be a set of N interest rates at time t with different maturities $\mathcal{T}_1<\cdots<\mathcal{T}_N$, Nelson and Siegel (1987) suggest the yield curve, i.e., a smooth function representing the interest rate or riskless zero-coupon bonds as a function of maturities $\mathcal{T}_i,\forall i\in\{1,2,\ldots,N\}$. Following Diebold and Li (2006) and allowing the β coefficients to vary over time, the yield curve based on the dynamic Nelson-Siegel model is given by:

$$y_t(\mathcal{T}_i)=\beta_{1t}+\beta_{2t}\left(\frac{1-e^{-\omega\mathcal{T}_i}}{\omega\mathcal{T}_i}\right)+\beta_{3t}\left(\frac{1-e^{-\omega\mathcal{T}_i}}{\omega\mathcal{T}_i}-e^{-\omega\mathcal{T}_i}\right)+\epsilon_{it}. \tag{7}$$

Diebold et al. (2006) treat $\boldsymbol{\beta}_t=(\beta_{1t},\beta_{2t},\beta_{3t})^\intercal$ as latent factors and represent the dynamic Nelson-Siegel model as a state space model:

$$\boldsymbol{y}_t=\boldsymbol{\Upsilon}(\omega)\boldsymbol{\beta}_t+\boldsymbol{\epsilon}_t,\qquad\boldsymbol{\epsilon}_t\sim\mathcal{N}(0,\boldsymbol{\Sigma}_\epsilon),\forall t\in\{1,2,\ldots T\}, \tag{8}$$

where $\boldsymbol{y}_t = [y_t(\mathcal{T}_1), \ldots, y_t(\mathcal{T}_N)]^\intercal$ are the observed interest rates at time t, $\boldsymbol{\epsilon}_t = [\epsilon_{1t}, \ldots, \epsilon_{Nt}]^\intercal$ denote the $i.i.d$ residuals, ω is a decay parameter, and the $N \times 3$ factor loading matrix is given by:

$$\boldsymbol{\Upsilon}_i = \left[1, \left(\frac{1 - e^{-\omega\mathcal{T}_i}}{\omega\mathcal{T}_i}\right), \left(\frac{1 - e^{-\omega\mathcal{T}_i} - \omega\mathcal{T}_i e^{-\omega\mathcal{T}_i}}{\omega\mathcal{T}_i}\right)\right]. \tag{9}$$

Assuming that $\boldsymbol{\beta}_t$ is following the vector autoregressive process, we have:

$$\boldsymbol{\beta}_{t+1} = (\mathbf{I} - \boldsymbol{\Psi})\boldsymbol{\mu} + \boldsymbol{\Psi}\boldsymbol{\beta}_t + \boldsymbol{\eta}_t, \qquad \boldsymbol{\eta}_t \sim \mathcal{N}(0, \boldsymbol{\Sigma}_\eta), \tag{10}$$

where $\boldsymbol{\mu}$ is a 3×1 vector of constants, $\boldsymbol{\Psi}$ is a 3×3 coefficient matrix, the covariance matrix of the disturbance vector, $\boldsymbol{\Sigma}_\eta$, is independent of the residuals $\boldsymbol{\epsilon}_t$. Choosing a covariance matrix for the β coefficients s.t. $\boldsymbol{\Sigma}_\eta = \boldsymbol{\Sigma}_\beta - \boldsymbol{\Psi}\boldsymbol{\Sigma}_\beta\boldsymbol{\Psi}^\intercal$, one can set the initial condition as $\boldsymbol{\beta}_1 \sim \mathcal{N}(\boldsymbol{\mu}, \boldsymbol{\Sigma}_\beta)$.

The dynamic Nelson-Siegel model presented in Eqs. (9)-(10) can be considered as a linear Gaussian state space model and the Kalman filter can be utilized to obtain the latent factors and estimate the parameters using the maximum likelihood estimation.

Let $\mathbf{b}_{t|l}$ be the minimum mean square linear estimator of β coefficients, $\mathbf{B}_{t|l}$ be the mean square error for $\mathbf{y}_1, \ldots, \mathbf{y}_l, l = t-1, t$. Utilizing the Kalman filtering, one first estimates:

$$\mathbf{b}_{t|t} = \mathbf{b}_{t|t-1} + \mathbf{B}_{t|t-1}\boldsymbol{\Upsilon}(\omega)^\intercal\mathbf{F}_t^{-1}\mathbf{v}_t, \mathbf{B}_{t|t} = \mathbf{B}_{t|t-1} + \mathbf{B}_{t|t-1}\boldsymbol{\Upsilon}(\omega)^\intercal\mathbf{F}_t^{-1}\boldsymbol{\Upsilon}(\omega)\mathbf{B}_{t|t-1}, \tag{11}$$

where $\mathbf{v}_t = \mathbf{y}_t - \boldsymbol{\Upsilon}(\omega)\mathbf{b}_{t|t-1}$ is the prediction error with the covariance matrix $\mathbf{F}_t = \boldsymbol{\Upsilon}(\omega)\mathbf{B}_{t|t-1}\boldsymbol{\Upsilon}(\omega)^\intercal + \boldsymbol{\Sigma}_\epsilon$. For time $t+1$, we have:

$$\mathbf{b}_{t+1|t} = (\mathbf{I} - \boldsymbol{\Psi})\boldsymbol{\mu} + \boldsymbol{\Psi}\mathbf{b}_{t|t}, \mathbf{B}_{t+1|t} = \boldsymbol{\Psi}\mathbf{B}_{t|t}\boldsymbol{\Psi}^\intercal + \boldsymbol{\Sigma}_\eta. \tag{12}$$

Setting the initial values $\mathbf{b}_{1|0} = \boldsymbol{\mu}$ and $\mathbf{B}_{1|0} = \boldsymbol{\Sigma}_\beta$, and $\boldsymbol{\Phi} = (\boldsymbol{\Psi}, \boldsymbol{\mu}, \omega, \boldsymbol{\Sigma}_\eta, \boldsymbol{\Sigma}_\epsilon)$, the log-likelihood function is given by:

$$\mathcal{L}(\boldsymbol{\Phi}) = -\frac{NT}{2}\log 2\pi - \frac{1}{2}\sum_{t=1}^{T}\log|\mathbf{F}_t| - \frac{1}{2}\sum_{t=1}^{T}\mathbf{v}_t^\intercal\mathbf{F}_t^{-1}\mathbf{v}_t. \tag{13}$$

2.3 Coupon-paying Bond Pricing

Although some studies have focused on bond portfolio optimization, most of them use pure discount/zero-coupon bonds (see e.g., Cheng, 1962; Roll, 1971; Korn and Koziol, 2006; Caldeira et al., 2016). More recently, Deguest et al. (2018) develop a portfolio optimization method for coupon-paying bonds including the duration constraint. We apply their methodology to first obtain future price, duration, and convexity for non-callable coupon-paying bonds. Then, applying the approach suggested in Dunetz and Mahoney (1988), we extend the pricing framework to callable bonds.

Let P_{jt} be the (dirty) price of coupon-paying bond $j \in \{1, 2, \ldots, d\}$ at time t, with known future coupon payments and dates. Let a_j denote the annualized interval for payments received from bond j with an annualized coupon rate of r_j^c, redemption (face) value of $\mathcal{V}_j$, payment dates $t_{j\mathcal{T}_{j1}}, \ldots, t_{j\mathcal{T}_{jM}}$, where $t_{j\mathcal{T}_M}$ is the redemption date and $\mathcal{T}_{j1}, \ldots, \mathcal{T}_{jM}$ are time to maturity for bond j cash flows. We can write the price of a coupon-paying bond as:

$$P_{jt} = \begin{cases} \sum_{m=k+1}^{\mathcal{T}_{jM}} a_j r_j^c \mathcal{V}_j \mathcal{B}(t, t_{j\mathcal{T}_{jm}}) + \mathcal{V}_j \mathcal{B}(t, t_{j\mathcal{T}_{jM}}), & t_{jk} \leq t < t_{j,k+1} \\ P_{jt^-} - a_j r_j^c \mathcal{V}_j & t = t_{jk}, \end{cases} \tag{14}$$

where the second condition is to deduct the cash payment from the bond price at the payment dates. Using the maturity-matched yields form the term structure modeled in Section 2.2, the price of a zero-coupon bond with a redemption value of 1 is given by:

$$\mathcal{B}(t, t_{j\mathcal{T}_{jm}}) = e^{-\mathcal{T}_{jm}[y_t(\mathcal{T}_{jm}) + s_{jt}]}, \tag{15}$$

where $y_t(\mathcal{T}_{jm})$ is the zero-coupon bond yield with life-to-maturity $\mathcal{T}_{jm}$ at time t, and s_{jt} is the coupon-paying bond yield spread.

The modified duration, i.e., the sensitivity of bond price $w.r.t.$ changes in interest rates, can be computed as the sum of maturity-weighted discounted payments:

$$\mathcal{D}_{jt} = \frac{1}{P_{jt}} \sum_{m=k+1}^{\mathcal{T}_{jM}} \mathcal{T}_{jm} a_j r_j^c \mathcal{V}_j \mathcal{B}(t, t_{j\mathcal{T}_{jm}}) + \mathcal{T}_{jM} \mathcal{V}_j \mathcal{B}(t, t_{j\mathcal{T}_{jM}}), t_{jk} \leq t < t_{j,k+1}. \tag{16}$$

The bond convexity, i.e., the sensitivity of bond duration $w.r.t.$ changes in interest rates computed as the second derivative of bond price $w.r.t.$ to interest rates, is given by:

$$\mathcal{C}_{jt} = \frac{1}{P_{jt}} \sum_{m=k+1}^{\mathcal{T}_{jM}} (\mathcal{T}_{jm}^2 + \mathcal{T}_{jm}) a_j r_j^c \mathcal{V}_j \mathcal{B}(t, t_{j\mathcal{T}_{jm}}) + (\mathcal{T}_{jM}^2 + \mathcal{T}_{jM}) \mathcal{V}_j \mathcal{B}(t, t_{j\mathcal{T}_{jM}}), t_{jk} \leq t < t_{j,k+1}. \tag{17}$$

To estimate option-adjusted price, duration, and convexity for a callable bond, let P_{jt}^{option} denote the price of the call option embedded in corporate bond j and time t. One can use typical option pricing models to obtain the value of the call, i.e., the Finite Difference method for American type and Black-Scholes model for European calls (see e.g., Hull and White, 1990). Following Dunetz and Mahoney (1988) and Vassiadou-Zeniou and Zenios (1996), we define the price of callable bonds as the difference between non-callable bond price and the call option price; $P_{jt}^{callable} = P_{jt} - P_{jt}^{option}$. Estimating the option Greeks, i.e., delta, Δ_{jt}, as well as, gamma, Γ_{jt}, from the option pricing model, Dunetz and Mahoney (1988) derive the bond's option-adjusted duration as:

$$\mathcal{D}_{jt}^{callable} = \frac{P_{jt}\mathcal{D}_{jt}(1-\Delta_{jt})}{P_{jt}^{callable}}, \tag{18}$$

and the option-adjusted convexity as:

$$\mathcal{C}_{jt}^{callable} = \frac{P_{jt}[\mathcal{C}_{jt}(1-\Delta_{jt}) - P_{jt}\Gamma_{jt}\mathcal{D}_{jt}^2]}{P_{jt}^{callable}}. \tag{19}$$

2.4 Multiobjective Bond Portfolio Optimization

In our portfolio optimization system, we apply linear programming to solve the multiobjective bond portfolio (MOBP) problem, with several attributes, including expected returns, CVaR, duration, convexity, distance-to-default, and turnover. We further extend these portfolio optimization systems to socially responsible investments and examine the impact of including ESG scores and CO2 emissions. In the suggested portfolio optimization, the objectives are weighted assuming known preference parameters for the investor. We first present a general multiobjective portfolio (MOP) problem presented in Sahamkhadam and Stephan (2024). Then, we extend this approach to our bond portfolios.

2.4.1 Multiobjective Portfolio Problem

Let $\Lambda_k(\hat{\mathbf{w}}_t)$ be a reward function and $\psi_q(\hat{\mathbf{w}}_t)$ be a risk measure. In the weighted-sum approach, the weights assigned to the objective functions, i.e., $\lambda_{\Lambda_k}, \lambda_{\psi_q} \in [0,1]$, correspond to the investor's preferences. Following Cao, Fuentes-Cortes, Chen and Zavala (2017), we apply the linear normalization (scaling) of the objective functions using the so-called utopia and nadir points. Let $\bar{\Lambda}_k$ and $\bar{\psi}_q$ denote the utopia solutions, and $\underline{\Lambda}_k$ and $\underline{\psi}_q$ are the nadir points. Using the weighted-sum approach, a MOP with $K+Q$ criteria is defined as:

$$\begin{aligned} \underset{\hat{\mathbf{w}}_t}{\text{minimize}} \quad & \sum_{q=1}^{Q} \lambda_{\psi_q} \left[\frac{\psi_q(\hat{\mathbf{w}}_t)}{\underline{\psi}_q - \bar{\psi}_q} \right] - \\ & \sum_{k=1}^{K} \lambda_{\Lambda_k} \left[\frac{\Lambda_k(\hat{\mathbf{w}}_t)}{\bar{\Lambda}_k - \underline{\Lambda}_k} \right] \\ \text{subject to} \quad & \hat{\mathbf{w}}_t^{\intercal}\mathbf{1} = 1 \\ & \hat{w}_{jt} \geq 0, \forall j \in \{1,2,..,d\} \end{aligned} \tag{20}$$

where $\sum_{q=1}^{Q}\lambda_{\psi_q} + \sum_{k=1}^{K}\lambda_{\Lambda_k} = 1$, and the utopia solutions are obtained from separate (individual) optimizations s.t. $\forall k \in \{1,2,\ldots,K\} : \bar{\Lambda}_k = \max_{\hat{\mathbf{w}}_t} \Lambda_k(\hat{\mathbf{w}}_{\Lambda_k})$ and $\forall q \in \{1,2,\ldots,Q\} : \bar{\psi}_q = \min_{\hat{\mathbf{w}}_t} \psi_q(\hat{\mathbf{w}}_{\psi_q})$. For nadir solutions, we have $\forall k \in \{1,2,\ldots,K\} : \underline{\Lambda}_k = \min\big(\Lambda_k(\hat{\mathbf{w}}_{\Lambda_1}),\ldots,\Lambda_k(\hat{\mathbf{w}}_{\Lambda_K}), \Lambda_k(\hat{\mathbf{w}}_{\psi_1}),\ldots,\Lambda_k(\hat{\mathbf{w}}_{\psi_Q})\big)$ and $\forall q \in \{1,2,\ldots,Q\} : \underline{\psi}_q = \max\big(\psi_q(\hat{\mathbf{w}}_{\Lambda_1}),\ldots,\psi_q(\hat{\mathbf{w}}_{\Lambda_K}), \psi_q(\hat{\mathbf{w}}_{\psi_1}), \ldots,\psi_q(\hat{\mathbf{w}}_{\psi_Q})\big)$. We approximate the nadir solutions using a set of feasible solutions obtained from

separate optimizations of each objective (reward/risk) functions in the MOP approach.

2.4.2 Bond Portfolio Attributes

Markowitz (1952) suggested that for a d-dimensional portfolio with asset returns $\hat{\mathbf{r}}_t = (\hat{r}_{1t}, \hat{r}_{2t}, ..., \hat{r}_{dt})$, asset weights $\hat{\mathbf{w}}_t = (\hat{w}_{1t}, \hat{w}_{2t}, ..., \hat{w}_{dt})$, and a $d \times 1$ vector of means for bonds' returns $\hat{\boldsymbol{\mu}}_t = (\hat{\mu}_{1t}, \hat{\mu}_{2t}, ..., \hat{\mu}_{dt})$ at time t (out-of-sample iteration that corresponds to t^{th} trading/rebalancing of the portfolio), the portfolio's expected return is $\hat{\mathbf{w}}_t^\intercal \hat{\boldsymbol{\mu}}_t$.

Rockafellar and Uryasev (2000) suggest a transformation of portfolio CVaR, $\text{CVaR}_\alpha(\hat{\mathbf{w}}_t)$, into a convex and continuously differentiable function $\mathcal{F}_\alpha(\hat{\mathbf{w}}_t, l)$ as

$$\mathcal{F}_\alpha(\hat{\mathbf{w}}_t, l) = l + \frac{1}{1-\alpha} \int_{\hat{\mathbf{r}}_t \in \mathbb{R}^d} [\mathfrak{f}(\hat{\mathbf{w}}_t, \hat{\mathbf{r}}_t) - l]^+ p(\hat{\mathbf{r}}_t) d\hat{\mathbf{r}}_t \tag{21}$$

where $\alpha \in (0, 1)$ denotes the confidence level for CVaR, $\mathfrak{f}(\hat{\mathbf{w}}_t, \hat{\mathbf{r}}_t)$ is the loss function from the simulated out-of-sample returns, $\hat{\mathbf{r}}_t$, with the probability density denoted by $p(\hat{\mathbf{r}}_t)$, and the objective is to minimize losses beyond the VaR threshold, $l \in \mathbb{R}$, s.t. $P[\mathfrak{f}(\hat{\mathbf{w}}_t, \hat{\mathbf{r}}_t) \geq \text{VaR}_\alpha(\hat{\mathbf{w}}_t)] = 1 - \alpha$, and $[\mathfrak{f}(\hat{\mathbf{w}}_t, \hat{\mathbf{r}}_t) - l]^+ = \max\{[\mathfrak{f}(\hat{\mathbf{w}}_t, \hat{\mathbf{r}}_t) - l], 0\}$.

By drawing M simulations from the probability distribution of $\hat{\mathbf{r}}_t$ according to $p(\hat{\mathbf{r}}_t)$, s.t. $\hat{\mathbf{r}}_t = \{\hat{\mathbf{r}}_{mt},\ m = 1, ..., M\}$, we can approximate $\mathcal{F}_\alpha(\hat{\mathbf{w}}_t, l)$ as:

$$\zeta_\alpha(\hat{\mathbf{w}}_t, l) = l + \frac{1}{M(1-\alpha)} \sum_{m=1}^{M} \big[\mathfrak{f}(\hat{\mathbf{w}}_t, \hat{\mathbf{r}}_{mt}) - l\big]^+. \tag{22}$$

Following Rockafellar and Uryasev (2000), we use the approximation presented in Eq. (22) to minimize CVaR. By setting $\mathfrak{f}(\hat{\mathbf{w}}_t, \hat{\mathbf{r}}_{mt}) = -\hat{\mathbf{w}}_t^\intercal \hat{\mathbf{r}}_{mt}$ and $l = \text{VaR}_\alpha(\hat{\mathbf{w}}_t)$ and introducing an auxiliary variable $\boldsymbol{\upsilon}_t = (\upsilon_{1t}, \upsilon_{2t}, ..., \upsilon_{Mt})$ such that $\boldsymbol{\upsilon}_{mt} = \big[-\hat{\mathbf{w}}_t^\intercal \hat{\mathbf{r}}_{mt} - \text{VaR}_\alpha(\hat{\mathbf{w}}_t)\big]^+$, we linearize $\zeta_\alpha(\hat{\mathbf{w}}_t, l)$.

One important aspect of bond investments is corporate credit risk. The general approaches available to investors for assessing the creditworthiness of a firm include (i) the ratings and default probabilities provided by rating agencies such as Moody's and Standard & Poor's, implemented in, e.g., JP Morgan's CreditMetrics framework; (ii) the distance-to-default measure based on the option-pricing framework proposed by Merton (1974) and extended by Black and Cox (1976), Longstaff and Schwartz (1995), and Afik, Arad and Galil (2016), among others (see Crouhy, Galai and Mark, 2000; Schaefer and Strebulaev, 2008, for a comparison of different approaches).

In Merton's distance-to-default approach, a firm's equity is considered a call option written on the underlying value of the firm, with an exercise price equal to the face value of the firm's debt. This approach assumes that both the firm's value and its volatility are inferred from the value of equity and that the probability of default follows a Gaussian cumulative density function dependent on the firm's underlying value, volatility, and debt (see Bharath and Shumway, 2008, for more details and formulations). In this paper, we use Merton's distance-to-default approach,

as it has been widely applied in practice and has demonstrated strong performance in empirical applications (Duffie, Saita and Wang, 2007; Jessen and Lando, 2015).

For investments in fixed-income assets such as corporate bonds, a portfolio manager should consider a major risk faced by investors: interest rate risk. To model the sensitivity of bond prices to interest rate changes, duration, and convexity measures are widely used in bond portfolio optimization Fabozzi (1999).

Although duration provides information on a bond's price sensitivity to interest rate changes, it assumes a linear price-yield relationship. In reality, the price-yield relationship exhibits a convex shape captured by the convexity measure. Duration can be considered an interest rate risk measure with a straightforward interpretation: it represents the sensitivity of a portfolio's value to interest rate changes and is minimized in bond portfolio management.

Regarding convexity, it can be either negative or positive when both non-callable and callable bonds are included in a portfolio. When convexity is positive, price appreciation exceeds price depreciation in response to large changes in yields. Conversely, negative convexity occurs when price appreciation is smaller than the price decline when interest rates decrease. Therefore, one could argue that, combined with duration minimization, positive convexity is more favorable for bond investors, as they benefit from price increases when yields change. [1]

We consider a linear form for bond portfolio duration, convexity, and distance-to-default. Let $\boldsymbol{\mathcal{D}}_t = (\mathcal{D}_{1t}, \ldots, \mathcal{D}_{dt})$, $\boldsymbol{\mathcal{C}}_t = (\mathcal{C}_{1t}, \ldots, \mathcal{C}_{dt})$, and $\mathbf{DtD}_t = (\mathrm{DtD}_{1t}, \ldots, \mathrm{DtD}_{dt})$ be the vectors containing bonds' modified (option-adjusted) durations and convexities, as well as distance-to-default. Considering a linear form for these attributes, we have $\hat{\mathbf{w}}_t^\intercal \boldsymbol{\mathcal{D}}_t$, $\hat{\mathbf{w}}_t^\intercal \boldsymbol{\mathcal{C}}_t$, and $\hat{\mathbf{w}}_t^\intercal \mathbf{DtD}_t$ as portfolio duration, convexity, and distance-to-default, respectively. Our optimization approach minimizes the portfolio duration and maximizes the portfolio convexity and distance-to-default.

The portfolio turnover is commonly used to estimate the transaction costs (see e.g., Steuer, Qi and Hirschberger, 2005, 2007). Following DeMiguel, Garlappi and Uppal (2009), we define the portfolio turnover as

$$\vartheta(\hat{\mathbf{w}}_t) = |\hat{\mathbf{w}}_t - \hat{\mathbf{w}}_{t^*}|^\intercal \mathbf{1} \tag{23}$$

where $\hat{\mathbf{w}}_{t^*}$ denotes a vector of asset weights at the end of the previous rebalancing period. For a long-only portfolio strategy, we have $\vartheta(\hat{\mathbf{w}}_t) \in [0, 2]$. To linearize $\vartheta(\hat{\mathbf{w}}_t)$, we use auxiliary variable $\mathbf{g}_t$, s.t. $\forall j \in \{1, 2, .., d\} : \hat{w}_{jt} - \hat{w}_{jt^*} + g_j \geq 0,\ \hat{w}_{jt^*} - \hat{w}_{jt} + g_j \geq 0$. [2]

To construct socially responsible multiobjective bond portfolios, we denote $\boldsymbol{\theta}_t = (\theta_{1t}, \theta_{2t}, ..., \theta_{dt})$ as a vector of ESG scores, the portfolio ESG score at time t is given by $\hat{\mathbf{w}}_t^\intercal \boldsymbol{\theta}_t$. Using the suggested

[1] In the current version of the paper, we consider maximizing convexity. However, one should note that this does not imply a reduction in sensitivity to interest rate risk. An alternative approach to be tested in further research is to define convexity as a risk measure. This can be done by formulating convexity as an absolute value function and incorporating it as a portfolio objective to be minimized. Therefore, the goal would be to reduce both negative and positive values of bond portfolio convexity.

[2] Rather than defining an upper boundary for portfolio turnover, we incorporate the turnover as an objective function to be minimized, with an optimal value of zero when $\hat{w}_{jt} = \hat{w}_{jt^*}$. Note that $\hat{\mathbf{w}}_{t^*}$ is fixed and given from the previous rebalancing period.

linear transformations of portfolios' CVaR and turnover, i.e., defining auxiliary variables $\boldsymbol{\upsilon},\ \mathbf{g}$, we obtain the socially responsible MOBP problem as:

$$
\begin{aligned}
\underset{\hat{\mathbf{w}}_t,\mathbf{g},\boldsymbol{\upsilon}}{\text{minimize}} \quad & \lambda_{\psi_\zeta}\left[\frac{l+[M(1-a)]^{-1}\sum_{m=1}^{M}\upsilon_m}{\underline{\psi}_\zeta-\bar{\psi}_\zeta}\right]+\lambda_{\psi_\mathcal{D}}\left[\frac{\hat{\mathbf{w}}_t^\intercal\boldsymbol{\mathcal{D}}_t}{\underline{\psi}_\mathcal{D}-\bar{\psi}_\mathcal{D}}\right]+ \\
& \lambda_{\psi_\vartheta}\left[\frac{\sum_{j=1}^{d}g_j}{\underline{\psi}_\vartheta-\bar{\psi}_\vartheta}\right]-\lambda_{\Lambda_\mu}\left[\frac{\hat{\mathbf{w}}_t^\intercal\boldsymbol{\mu}_t}{\bar{\Lambda}_\mu-\underline{\Lambda}_\mu}\right]-\lambda_{\Lambda_\mathcal{C}}\left[\frac{\hat{\mathbf{w}}_t^\intercal\boldsymbol{\mathcal{C}}_t}{\bar{\Lambda}_\mathcal{C}-\underline{\Lambda}_\mathcal{C}}\right]- \\
& \lambda_{\Lambda_{\text{DtD}}}\left[\frac{\hat{\mathbf{w}}_t^\intercal\text{DtD}_t}{\bar{\Lambda}_{\text{DtD}}-\underline{\Lambda}_{\text{DtD}}}\right]-\lambda_{\Lambda_\theta}\left[\frac{\hat{\mathbf{w}}_t^\intercal\boldsymbol{\theta}_t}{\bar{\Lambda}_\theta-\underline{\Lambda}_\theta}\right], \\
\text{subject to} \quad & -\hat{\mathbf{w}}_t^\intercal\hat{\mathbf{r}}_{mt}+l+\upsilon_m\geq 0 && \forall m\in\{1,2,..,M\}, \\
& \hat{w}_{jt}-\hat{w}_{jt^*}+g_j\geq 0 && \forall j\in\{1,2,..,d\}, \\
& \hat{w}_{jt^*}-\hat{w}_{jt}+g_j\geq 0 && \forall j\in\{1,2,..,d\}, \\
& \hat{\mathbf{w}}_t^\intercal\mathbf{1}=1, \\
& \upsilon_m\geq 0 && \forall m\in\{1,2,..,M\}, \\
& \hat{w}_{jt}\geq\frac{1}{\kappa d} && \forall j\in\{1,2,..,d\}, \\
& -\hat{w}_{jt}\geq-\frac{\kappa}{d} && \forall j\in\{1,2,..,d\},
\end{aligned}
\tag{24}
$$

where the portfolio weights at the end of the previous rebalancing period $\hat{w}_{jt^*}$, the preference parameters $\boldsymbol{\lambda}_\psi$ and $\boldsymbol{\lambda}_\Lambda$, utopia solutions $\bar{\boldsymbol{\psi}}$ and $\bar{\boldsymbol{\Lambda}}$, and nadir solutions $\underline{\boldsymbol{\psi}}$ and $\underline{\boldsymbol{\Lambda}}$ are given, and the parameters to be estimated are the portfolio weights $\hat{\mathbf{w}}_t$ at time t (out-of-sample iteration) and auxiliary variables $\mathbf{g}$, and $\boldsymbol{\upsilon}$, with $2M+4d+1$ constraints. The last two constraints are enforced to avoid concentrated solutions and ensure a minimum level of diversification given the magnitude of the parameter κ (see Jagannathan and Ma, 2003; Deguest et al., 2018, for more details).

2.5 Copula-based MOBP Portfolio Optimization

In our copula-based forecasting approach, we estimate the returns' conditional multivariate distribution by following a series of steps. First, using the dynamic Nelson-Siegel model, the standardized residuals $\mathbf{z}$ and their marginal densities f_i are obtained. Then, using the marginal uniforms obtained from the probability transformation, a joint distribution for the term structure is estimated using the truncated Rvine density function. After that, drawing observations from the joint distribution and utilizing the step-ahead mean and volatility forecasts from the dynamic Nelson-Siegel model, the copula-based multivariate distribution is obtained. Having obtained the forecasts and simulations for the bonds yield curve, we estimate the no-arbitrage step-ahead prices, duration, and convexity for both zero-coupon and coupon-paying bonds, as well as for callable bonds. Finally, we use the simulated prices to solve the MOBP optimization problem and

obtain the bonds' portfolio optimal weights.

We set the following parameters: T = the total number of observations, L = the estimation window length, $\forall \iota \in [L+1, T]$: t_ι = out-of-sample iteration which also corresponds to the portfolio rebalancing periods, M = the total number of drawings from the step-ahead multivariate conditional return distribution, N = the total number of interest rates in the term structure, and d = the total number of assets in the portfolio. Repeat the following steps for all out-of-sample iterations $t_\iota = (t_{L+1}, t_{L+2}, \ldots, t_T)$:

Step 1. Initialize by setting $\forall t \in [t_{\iota-L}, t_{\iota-1}]$: $\boldsymbol{y}_t = [y_t(\mathcal{T}_1), \ldots, y_t(\mathcal{T}_N)]^\intercal$ as the zero-coupon yields.

Step 2. Fit the dynamic Nelson-Siegel model in Eqs. (7)-(13) to $\boldsymbol{y}_t$ and estimate the factor loadings in $\boldsymbol{\Upsilon}(\omega)$ and obtain one-step ahead forecasts for $\boldsymbol{\beta}_{t+1}$ using the Kalman filter and maximum likelihood estimation. Also, obtain standardized residuals $\hat{\mathbf{z}}_i = (\hat{z}_{it_{\iota-L}}, ..., \hat{z}_{it_{\iota-1}})$ using the (diagonal) covariance matrix $\boldsymbol{\Sigma}_\epsilon$.

Step 3. Utilize the estimated standardized residuals $\hat{z}_{it}$ from Step 2 and obtain uniform marginals $\hat{u}_{it} = F_i(\hat{z}_{it}),\ i \in [1, N],\ t \in [t_{\iota-L}, t_{\iota-1}]$ from the cumulative marginal distribution function s.t. $\hat{u}_{it} \sim U[0,1]^N$.[3]

Step 4. Insert the estimated marginal uniform $(\hat{U}_1, ..., \hat{U}_N)$ of step 3 into the truncated Rvine copula model in Eqs. (4)-(6) and estimate the copula parameter vector $\hat{\boldsymbol{\Omega}}$ using the maximum likelihood estimation.

Step 5. Draw M (e.g. 10000) uniform random numbers from the estimated multivariate Rvine copula distribution in step 4. Convert the simulated random numbers into standardized residuals $\hat{\tilde{\boldsymbol{z}}}_t = \{\hat{\tilde{\boldsymbol{z}}}_{mt},\ m = 1, ..., M,\ t = t_\iota\}$ using the inverse of the marginal distribution for each asset.

Step 6. Utilize the one-step ahead forecasts $\boldsymbol{\beta}_{t+1}$, factor loading $\boldsymbol{\Upsilon}(\omega)$ and covariance $\boldsymbol{\Sigma}_\epsilon$ from step 2 and simulated standard residuals $\hat{\tilde{\boldsymbol{z}}}_i$ from step 5, and obtain yield curve forecasts as $\hat{\mathbf{y}}_{mt} = \boldsymbol{\Upsilon}(\omega)\boldsymbol{\beta}_{t+1} + \hat{\tilde{\boldsymbol{z}}}_{mt}\boldsymbol{\Sigma}_\epsilon^{-1},\ \forall m \in [1, M],\ t = t_\iota$.

Step 7. $\forall j \in [1, d],\ \forall m \in [1, M],\ t = t_\iota$ Utilize the observed information, i.e., annualized cash flow interval a_j, annualized coupon rate r_j^c, redemption (face) value $\mathcal{V}_j$, payment dates $t_{j\mathcal{T}_{j1}}, \ldots, t_{j\mathcal{T}_{jM}}$, yield spread s_{jt}, and the price of the maturity-matched zero-coupon bonds $\mathcal{B}(t, t_{j\mathcal{T}_{jm}})$ in Eqs.14-19 and obtain M simulated step-ahead prices $\hat{\mathbf{P}}_t = \{\hat{\mathbf{P}}_{mt}, m = 1, \ldots, M\}$, duration $\hat{\boldsymbol{\mathcal{D}}}_t$ and convexity $\hat{\boldsymbol{\mathcal{C}}}_t$ for both non-callable and callable bonds.

Step 8. Given the observed prices at time $t_{\iota-1}$ and simulated prices $\hat{\mathbf{P}}_t$ from step 7, calculate the bond returns as $\hat{r}_{jt} = ln(\hat{p}_{jm}/p_{jt_{\iota-1}}),\ \forall j \in [1, d],\ \forall m \in [1, M]$

[3] We use the probability distribution function for the univariate Kernel density to transform standardized residuals to uniform marginals (see Nagler, 2024).

Step 9. Given the chosen MOBP and return forecasts $\hat{\mathbf{r}}_t = \{\hat{\mathbf{r}}_{mt},\ m = 1, ..., M\}$ from Step 8, estimate the utopia and nadir solutions for each portfolio objective, i.e. $\underline{\psi}_{\zeta}, \bar{\psi}_{\zeta}, \underline{\psi}_{\mathcal{D}}, \bar{\psi}_{\mathcal{D}}, \underline{\psi}_{\vartheta}, \bar{\psi}_{\vartheta}$, $\bar{\Lambda}_{\mu}, \underline{\Lambda}_{\mu}, \bar{\Lambda}_{\mathcal{C}}, \underline{\Lambda}_{\mathcal{C}}, \bar{\Lambda}_{\text{DtD}}, \underline{\Lambda}_{\text{DtD}}, \bar{\Lambda}_{\theta}, \underline{\Lambda}_{\theta}$.

Step 10. Insert the return forecasts $\hat{\mathbf{r}}_t = \{\hat{\mathbf{r}}_{mt},\ m = 1, ..., M\}$ from Step 8, utopia and nadir solutions from Step 9, and predefined preference parameters $\lambda_{\Lambda_{\mu}},\ \lambda_{\psi_{\zeta}},\ \lambda_{\Lambda_{\theta}},\ \lambda_{\psi_{\mathcal{D}}},\ \lambda_{\Lambda_{\mathcal{C}}},\ \lambda_{\Lambda_{\text{DtD}}},\ \lambda_{\psi_{\vartheta}}$ into the chosen MOBP optimization (Eq. 24) and estimate optimal asset weights $\hat{\mathbf{w}}_t = (\hat{w}_{1t}, \hat{w}_{2t}, ..., \hat{w}_{dt})$.

Step 11. Given the proportional transaction cost Γ and realization of asset returns from observed prices $\mathbf{r}_t$, register the portfolio return $R_t = [1 - \Gamma \sum_{j=1}^{d} (|\hat{w}_{jt} - \hat{w}_{jt^*}|)](1 + \hat{\mathbf{w}}_t^{\intercal} \mathbf{r}_t) - 1,\ t = t_{\iota}$.

2.6 Benchmark Portfolio Strategies

To benchmark the performance of the suggested copula-based Nelson-Siegel yield curve approach, we use a simpler version of the model, where the zero-coupon yields are simulated from the dynamic Nelson-Siegel factor model with a Gaussian marginal distribution, as assumed in the original model. Therefore, we replace steps 3–5 in Section 2.5 with simply simulating one-step-ahead zero-coupon yields and continue with the other steps. By doing so, we can identify possible benefits from modeling the nonlinear dependence structure between zero-coupon yields via R-vine copulas in terms of portfolio performance, as well as risk-adjusted returns. On the other hand, to benchmark the suggested MOBP portfolio optimization system, we apply a simple equally weighted (EQW) portfolio strategy.

3 Data

To construct and analyze the ESG-bond portfolios, we use a sample of 879 corporate ESG bonds collected from Thomson Reuters Refinitiv's Screener on July 5, 2024. The sample includes ESG bonds (i) with a public issuer, (ii) traded in the Euro currency, (iii) with fixed and zero (but not floating-rate) coupons and available coupon schedule, (iv) with maturity of more than one year but not perpetual, (v) with both non-callable and callable options (only European and American call type).

Figures 1-4 provides the distribution of the ESG bonds included in our sample concerning coupon, ESG, callable, call option, The Refinitiv Business Classification (TRBC), issue market, and country of domicile. While only 47 zero-coupon bonds were included in the sample, the vast majority (832) of the ESG bonds have fixed coupons. Of the 879 ESG bonds, 486 are Climate Bonds Initiative (CBI) aligned green bonds and 146 are self-labeled green bonds. Furthermore, our sample includes 455 callable bonds, of which, 439 have the American call option type, meaning that they can be redeemed by the issuer at any time until maturity. As regards economic sectors, more

(fewer) ESG bonds are issued by firms in the financials and utilities (healthcare and technology) sectors. While the majority (630) are Eurobonds, there are 226 domestic and 23 foreign bonds included in the sample. As regards the country of domicile, France, Germany, and the Netherlands are the countries with the highest number of corporate ESG bond issues traded in the Euro.

As discussed in Section 2, to forecast no-arbitrage step-ahead prices for the corporate bonds, both zero-coupon and fixed-coupon, we first model the term structure of short/long-term interest rates. Therefore, we collect the daily yields for zero-coupon governmental bonds from Germany, as representatives of EU interest rates, with maturities of 1, 3, 6, 9 months and 1-10, 12, 15, 20, 25, and 30 years, from January 31, 2014 until July 5, 2024. Moreover, we compute the dirty prices using clean prices and accrued interests collected by Thomson Reuters' Datastream. Other information from Datastream used to price the corporate bonds includes coupon schedule, i.e., coupon amounts and payment dates; redemption values; call schedule, i.e., call dates and values; life-to-maturity; and spread-over-benchmark. All series span over a period starting on January 31, 2014, and ending on July 5, 2024.

4 Empirical Analysis

To evaluate the suggested copula-based dynamic Nelson-Siegel model, we first perform an in-sample analysis of the latent factors estimated from the term structure model. Then in Section 4.2, we investigate the dependence structure within the yield curve. To estimate the dependence structure, we apply the truncated Rvine copula model and allow for several copula families to be selected, including Elliptical, i.e., Gaussian (symmetric no tail dependence), and Student-t (symmetric lower and upper tails), Archimedean, i.e., Clayton (asymmetric lower tail), Gumbel (asymmetric upper tail), Frank, Joe (asymmetric upper tail), Clayton-Gumbel (BB1, asymmetric lower and upper tails), Joe-Gumbel (BB6, asymmetric upper tail), Joe-Clayton (BB7, asymmetric lower and upper tails);, Joe-Frank (BB8, asymmetric upper tail), and non-parametric, i.e., Transformation Local Likelihood Kernel (TLL) (see Nagler and Vatter, 2021, for more details on copula families). Furthermore, we allow for truncation based on the mBICV criterion, as well as rotated copula families.

To evaluate the suggested MOBP strategies, we perform portfolio out-of-sample optimization and back-testing. To do so, we apply a rolling window estimation where we use a training sample of 500 days and fit the copula-based dynamic Nelson-Siegel model to the EU yield curve, estimate one-step ahead conditional distribution, and simulate step-ahead zero-coupon yields. Using these yields, we forecast and obtain a conditional distribution for the no-arbitrage dirty prices and returns for the ESG bonds included in our sample. Using these simulated returns and other information, i.e., (option-adjusted) duration and convexity, as well as distance-to-default, and issuer ESG scores, we solve the suggested multiobjective portfolio problem numerically and obtain the

optimal weights. We repeat this process for each out-of-sample iteration. Using observed total returns, collected from Thomson Reuters' Refinitiv Eikon, and the estimated portfolio weights, based on a daily re-balancing strategy, we compute the portfolio returns. Finally, we compare the out-of-sample performance, in terms of risk-adjusted ratios and economic performance, of the suggested MOBPs with the equally weighted benchmark.

In the suggested MOBP approach, the κ parameter is included to enforce a minimum level of diversification. Lowering the κ parameter, but not below one, leads to portfolio weights closer to that of the equally weighted portfolio. Following Deguest et al. (2018), we start our portfolio performance analysis by setting the κ to 4. As a robustness check, we change the κ to 2 and 10 and perform out-of-sample optimization and back-testing. In addition, to construct socially responsible portfolios, we include the bonds' issuer ESG ratings and define the portfolio ESG score as one of the portfolio attributes. We perform a robustness check, use the issuer CO2 emissions in level, and investigate whether minimizing CO2 emissions, as a portfolio risk measure, would be at the cost of reducing portfolio risk-adjusted ratios and economic performance.

4.1 The EU Term Structure

We start our empirical analysis by analyzing the latent factors, i.e., level, slope, and curvature (shape) of the EU yield curve obtained utilizing the parsimonious and flexible Nelson-Siegel term structure model. In doing so, we use daily yields for 19 German zero-coupon governmental bonds with different maturities, over 10 years from January 2014 to July 2024, and fit the dynamic Nelson-Siegel model described in Section 2.2 to the whole sample and estimate the parameters and latent factors using the Kalman filter and the Maximum Likelihood Estimation.

Figure 5 plots the in-sample estimation of the three latent factors. The level factor shows a decline in all yield until 2021 due to the reduction of interest rates posed by the European Central Bank as a response to the EU Sovereign debt crisis, and a gradual rise until 2024 due to the inflationary environment caused by the Russo-Ukraine war. The slope follows an ascending pattern with negative values as expected. Similarly, the curvature (shape) is mostly negative except for the 2022-2023 period and is highly (positively) correlated with the slope. As expected, the curvature displays higher variation than the slope and level factors.

4.2 Yield Curve Dependence Structure

This section investigates the dependence structure among interest rates with different maturities. Having estimated the term structure model, we obtain standardized residuals in Eqs. (7)-(8) and transform them into uniform marginals. Using these uniform marginals, we estimate the dependence structure based on the truncated Rvine copula model described in Section 2.1.

Figures 6-7 provide pair-wise plots and histograms for the uniform marginals. The near-term

yields generally show high correlations and high degrees of tail dependence, both upper and lower. For instance, considering the pair-wise plot between the two-year and three-year zero-coupon yields, there exists high tail dependence both in the lower and upper sides, which can be captured by a copula family capturing dependence at the two tails, e.g., Student-t, BB1 or BB7. Another example of asymmetric tail dependence is illustrated in the par-wise plot between the 12-year and 15-year yields. On the other hand, between the zero-coupon yields with distanced maturities, there are low degrees of dependencies. For instance, the pair-wise plot between 7-year and 30-year yields shows no dependence with an estimated Kendall's τ of 0.0095. As shown in Figure 6, there are instances in a rotated copula family that are useful in capturing the dependence structure, e.g., between one-month and nine-month yields. Overall, our results indicate that (i) the assumption that deviations from the yield curve are uncorrelated is only valid for zero-coupon yields with distanced maturities, and (ii) there exists tail dependency among the yields that can motivate the application of symmetric and asymmetric tail dependence modeling when forecasting the interest rates.

Having established the intuition of dependence modeling for the yield curve, we apply the truncated Rvine copula model. Figures 8-12 show the first five vine trees estimated using the Rvine structure, with zero-coupon yields with different maturities placed at the edges, and bivariate copula families, along with Kendall's τ in parentheses, are at the nodes. As shown in Figure 8, the 3-month and 5-year yields show the highest correlations with other yields and are placed at the center of the dependence structure. The Student-t and mixture copulas such as BB1 and BB7 are selected more frequently. Moving to the fifth tree in Figure 12, the estimated Kendall's τ has a lower value, indicating less dependency observed in higher trees and, therefore, the plausibility of truncating the vine structure.

4.3 Tri-criteria Pareto Frontiers

To establish the bond portfolio performance regarding different attributes, we perform an in-sample analysis of the efficient frontiers when there are three portfolio objectives. In doing so, we use a sample of ESG bond observed total returns over 500 days from August 8, 2022, until July 5, 2024, during which there are 543 available ESG bonds in our sample. We utilize the estimates for the (option-adjusted) duration and convexity in Eqs. (16)-(19), as well as distance-to-default, along with the observed total returns and bond issuer's ESG scores from Thomson Reuters' Refinitiv. We obtain optimal weights for the tri-criteria MOBPs by changing the investor preference parameters λ. We provide the results only for cases when expected return and CVaR are two of the portfolio objectives and add either duration, convexity, distance-to-default, or ESG scores as the third objective. [4]

[4]To construct the Pareto frontiers, we impose long-only constraints for the portfolio weights, i.e., $\hat{w}_{jt} \geq 0 \ \ \forall j \in \{1, 2, .., d\}$. This is to obtain the full Pareto frontiers.

Figure 13 plots the Pareto frontiers. In most cases, the Pareto frontier shows a triangular surface with corner solutions representing the utopia (best optimal) points for each portfolio objective. This indicates that these portfolio attributes are less correlated and can be included in a multiobjective portfolio problem. Furthermore, in all panels, the concentration of the Pareto points happens close to an expected return between zero and 0.04% and a CVaR between 0.5% and 1%. In Panel (i), most of the portfolios on the Pareto frontier achieve an ESG score of at least 80 due to high ESG ratings for the issuers of ESG bonds.

4.4 MOBPs Out-of-sample Performance

To evaluate the out-of-sample performance of the suggested copula-based extension of the dynamic Nelson-Siegel model and the MOBP optimization, we construct multiobjective strategies by adding different attributes to the classical mean-CVaR portfolio problem and set equal weights on each objective, that is, equal preference parameters. In this case, each objective is equally important to the investor. To avoid concentrated solutions, we set the κ parameter to 4. Therefore, depending on the number of assets d included at each iteration, we set a minimum and maximum limit for the portfolio weights.

Table 1 reports the out-of-sample performance for the suggested MOBPs. In Panel (A), the equally-weighted benchmark achieves an annualized average return of 0.862% during the 2016-2024 period, with a volatility of 3.471% and a Sharpe ratio of 0.248. When using equal weights for the ESG bonds included in our sample, the resulting portfolio strategy leads to an ESG score of 75.7 indicating that the bond issuers are highly rated concerning their environmental, social, and governance performance. While the duration for the EQW portfolio is positive (3.852), it has a negative convexity due to the inclusion of callable bonds where price sensitivity to rising yields can increase. In Panel (A.1), the dynamic Nelson-Siegel portfolios achieve lower volatility and tail risk compared to the EQW portfolio, however, at the cost of reducing portfolio returns and wealth. Similar results are found for the socially responsible dynamic Nelson-Siegel portfolios when the inclusion of the ESG criteria increases the overall ESG score of the portfolios. In general, the results for benchmark portfolios indicate the benefits of applying the dynamic Nelson-Siegel latent factor approach in pricing corporate bonds, resulting in less risky bond portfolios. These results are in accordance with those found in previous studies such as Tu and Chen (2018) and Caldeira et al. (2016).

In Panel (B), all the suggested copula-based MOBPs achieve higher Sharpe ratios and lower standard deviations than both the EQW and the corresponding dynamic Nelson-Siegel benchmarks. As regards tail risk, all MOBPs reduce CVaR with the lowest reported for the three-criteria portfolio with mean, CVaR, and duration objectives ($\lambda_{\Lambda_\mu} = \lambda_{\psi_\varsigma} = \lambda_{\psi_\mathcal{D}} = 1/3$). This portfolio strategy also achieves the lowest duration, i.e., 2.517. When including the convexity,

$\Lambda_{\mathcal{C}}$, as one of the objectives, the portfolio results in a positive convexity that is more favorable for investors as a positive convexity for bond portfolios entails larger price increases due to a decline in yields than price declines due to a rise in yields. In Panel (C), we report the results for socially responsible copula-based MOBPs when including the ESG scores, Λ_{θ}, as an extra objective. In general, the socially responsible MOBPs achieve similar results, i.e., all portfolios outperform the EQW benchmark in terms of downside risk (CVaR) and risk-adjusted ratios (SR and STARR). However, these portfolios achieve only slightly higher ESG scores. Our intuition for these results is that the ESG bonds in the portfolios already have high issuer ESG scores. We will provide more results when including CO2 emissions as an alternative portfolio objective in Section 4.5. Considering economic performance, the MOBP with all seven objectives ($\lambda_{\Lambda_{\mu}} = \lambda_{\psi_{\zeta}} = \lambda_{\Lambda_{\theta}} = \lambda_{\psi_{\mathcal{D}}} = \lambda_{\Lambda_{\mathcal{C}}} = \lambda_{\Lambda_{\text{DtD}}} = \lambda_{\psi_{\vartheta}} = 1/7$), achieves a higher accumulated wealth, i.e., €113 and a lower average turnover of 0.058, compared to other MOBP strategies.

Figures 14-16 plot the wealth trajectory for the suggested copula-based MOBPs with different combinations of portfolio objectives and equal preference parameters. For both cases with and without ESG scores, most copula-based MOBPs achieve higher accumulated wealth during the aftermath of the Russo-Ukraine war compared to both the EQW and the corresponding dynamic Nelson-Siegel benchmarks. In particular, during the COVID-19 and Russo-Ukraine market turmoils, these MOBPs show more resilience than the benchmark strategies.

4.5 Robustness Checks

As a robustness check, we investigate whether changing the κ parameter affects the MOBP's out-of-sample performance. Tables 2-3 provide the results. Setting the κ to 2, we impose harder restrictions on the portfolio weights resulting in an average maximum weight between 2.8% and 3.8&, which is below that reported in Table 1 when $\kappa = 4$. Although, all MOBPs achieve higher returns when imposing a more restrictive level of diversification in Table 2 compared to the less restive cases, e.g.,$\kappa = 4$ and $\kappa = 10$ in Table 3, this at the cost of increasing both standard deviations and downside risk. On the other hand, when setting the κ parameter to 10, allowing for more concentrated portfolio weights, e.g., an average maximum weight of almost %13, we see a considerable reduction in the portfolio standard deviation and CVaR. These results indicate the investment risk reduction achieved when applying the suggested copula-based dynamic Nelson-Siegel model.

As discussed above, including the bond issuer ESG scores as a portfolio objective improves the portfolio ESG narrowly. As an alternative, we perform a robustness check and utilize the issuer's overall Carbon dioxide and CO2 equivalent emissions in level, i.e., Scope 1 plus Scope 2, as a criterion for constructing socially responsible portfolios. Table 4 reports the results for the MOBPs with CO2 emissions. In Panel (A), the EQW portfolio results in an average CO2

emission of 10,763,533 tonnes. However, when including the CO2 portfolio objective, this average reduces to less than 5 million tonnes for the MOBPs, while improving the portfolio performance as regards average returns and risk-adjusted ratios. Comparing the performance of MOBPs with CO2 criteria with those obtained based on the ESG scores in Panel (C) of Table 1, we find that the inclusion of portfolio CO2 emission as an alternative to ESG, in general, leads to socially responsible portfolios with higher average returns but at the cost of higher portfolio risk, e.g., standard deviation and CVaR. As shown in Figure 16, the MOBPs with CO2 emissions show more resilience during the market turmoils compared to the EQW benchmark and achieve higher accumulated wealth during the aftermath of market downturns. Overall, these results indicate that for the ESG bond portfolios, the CO2 emission can be utilized as an objective to achieve a more sustainable portfolio, i.e., less CO2 emission, that still outperforms the EQW benchmark concerning the classical risk and return measurements.

5 Conclusions

This paper introduces a comprehensive pricing framework for zero-coupon and fixed-coupon bonds, including both callable and non-callable variants. The dynamic Nelson-Siegel model is employed to forecast zero-coupon governmental bond yields, while an R-vine copula model captures the dependence structure between these yields. Additionally, a multi-objective bond portfolio optimization (MOBP) system is developed, integrating key criteria such as average return, Conditional Value-at-Risk (CVaR), duration, convexity, distance-to-default, ESG scores, and portfolio turnover.

The findings demonstrate that the proposed copula-based dynamic Nelson-Siegel framework effectively reduces portfolio risk and enhances risk-adjusted performance, particularly during periods of market stress such as the COVID-19 pandemic and the Russo-Ukrainian war. These results remain robust across different levels of portfolio diversification. Furthermore, the MOBP optimization approach offers investors flexibility in constructing ESG-focused bond portfolios tailored to their specific risk-return preferences.

A robustness check incorporating CO2 emissions as an alternative portfolio criterion to ESG scores shows that portfolios prioritizing lower carbon footprints achieve significant emissions reductions while maintaining superior return and risk performance compared to an equally weighted (EQW) benchmark.

Overall, this study highlights the copula-based dynamic Nelson-Siegel model as a reliable tool for bond return forecasting and ESG bond portfolio optimization, providing asset managers with a risk-sensitive and adaptable strategy for sustainable investing.

Several avenues for future research emerge. One potential extension is the application of copula modeling to alternative term structure models. Another is the construction of mixed-asset portfolios, as existing literature suggests that green bonds can serve as effective diversifiers. Additionally, integrating investor views through the Black-Litterman model could further refine bond portfolio optimization. Finally, the use of deep learning techniques to enhance yield curve forecasting presents an exciting opportunity for further innovation in fixed-income modeling.

Figures and Tables

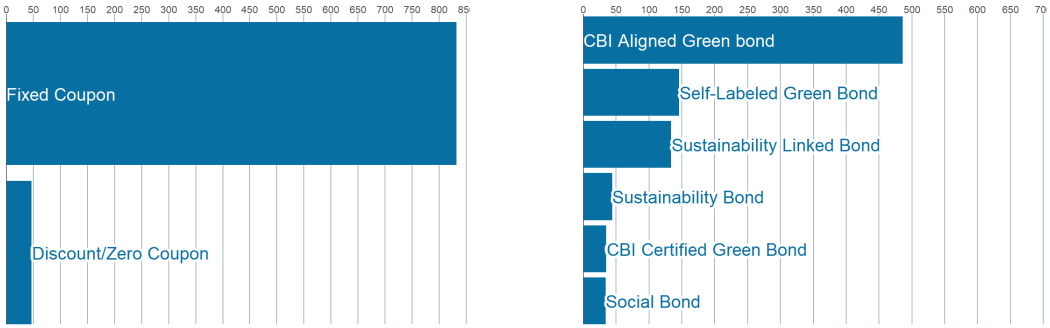

(a) (b)

Figure 1: This figure illustrates the number of bonds with different (a) coupon and (b) ESG types. The sample includes 879 ESG bonds, collected on July 5, 2024.

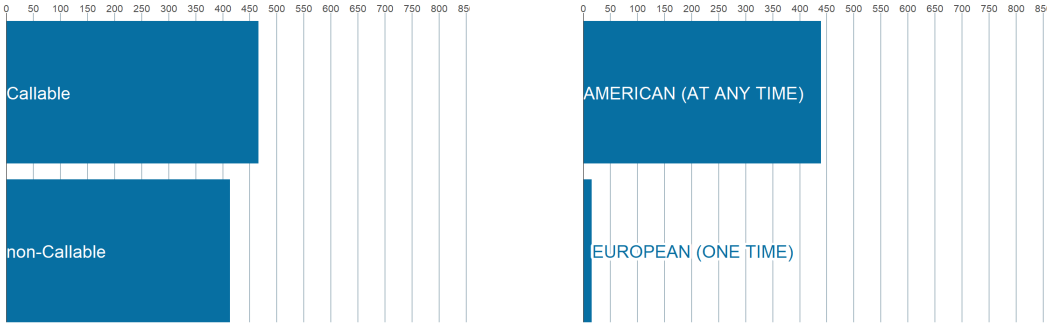

(a) (b)

Figure 2: This figure illustrates the number of bonds with different (a) call and (b) call option types. The sample includes 879 ESG bonds, collected on July 5, 2024.

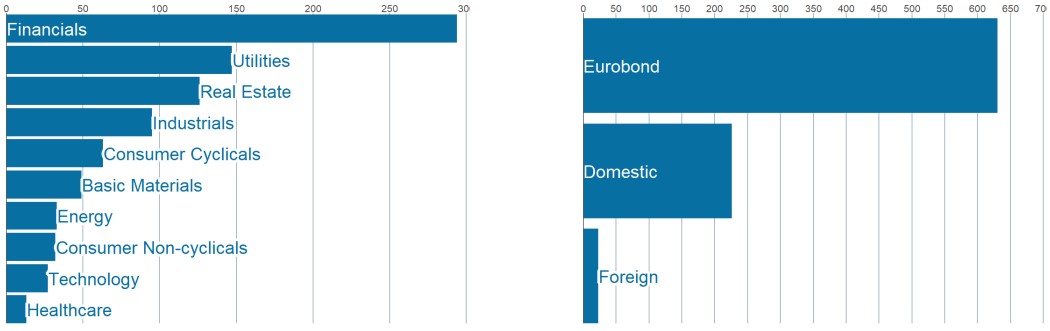

(a) (b)

Figure 3: This figure illustrates the number of bonds with different (a) TRBC economic sectors and (b) market of issue. The sample includes 879 ESG bonds, collected on July 5, 2024.

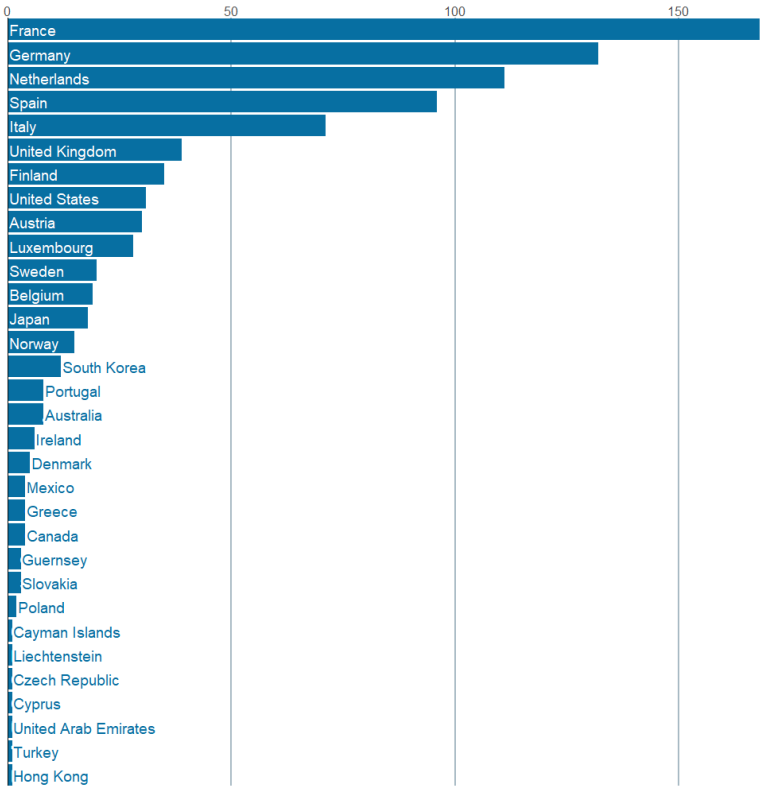

Figure 4: This figure illustrates the number of bonds with different country of domicile. The sample includes 879 ESG bonds, collected on July 5, 2024.

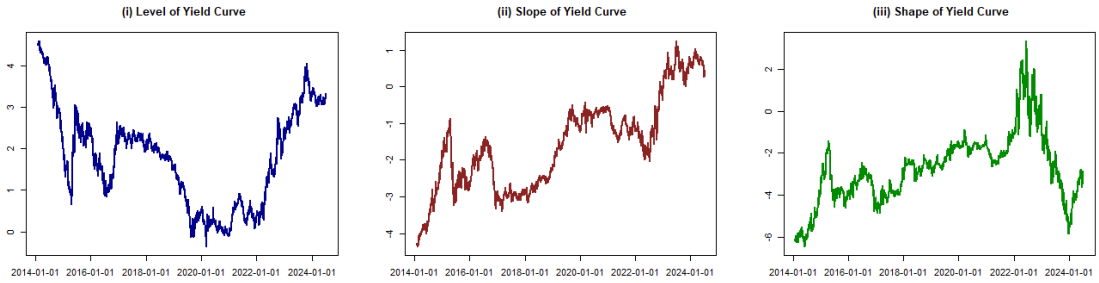

Figure 5: This figure plots the latent factors, i.e. level, slope, and shape of the term structure, from the dynamic Nelson-Siegel model estimated using the Kalman filter in Eqs. (7)-(13). The sample includes the daily yields for 19 governmental zero-coupon bonds from Germany, with maturities of one month to thirty years, from January 31, 2014, until July 5, 2024.

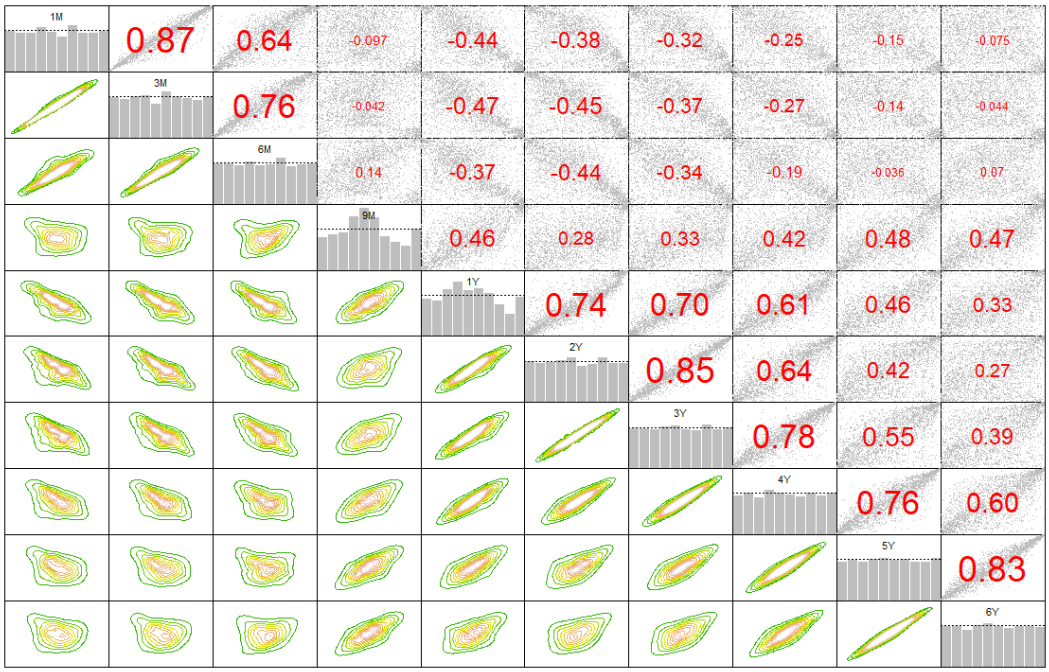

Figure 6: This figure illustrates the pairwise plot of uniform marginals for the yield curve for Germany. The uniform marginals are obtained based on probability transformation (univariate Kernel density) of standardized residuals from the dynamic Nelson-Siegel model in Eqs. (7)-(8). The sample includes daily governmental zero-coupon bond yields, with maturities of one month (1M) to thirty years (30Y), from January 31, 2014, until July 5, 2024.

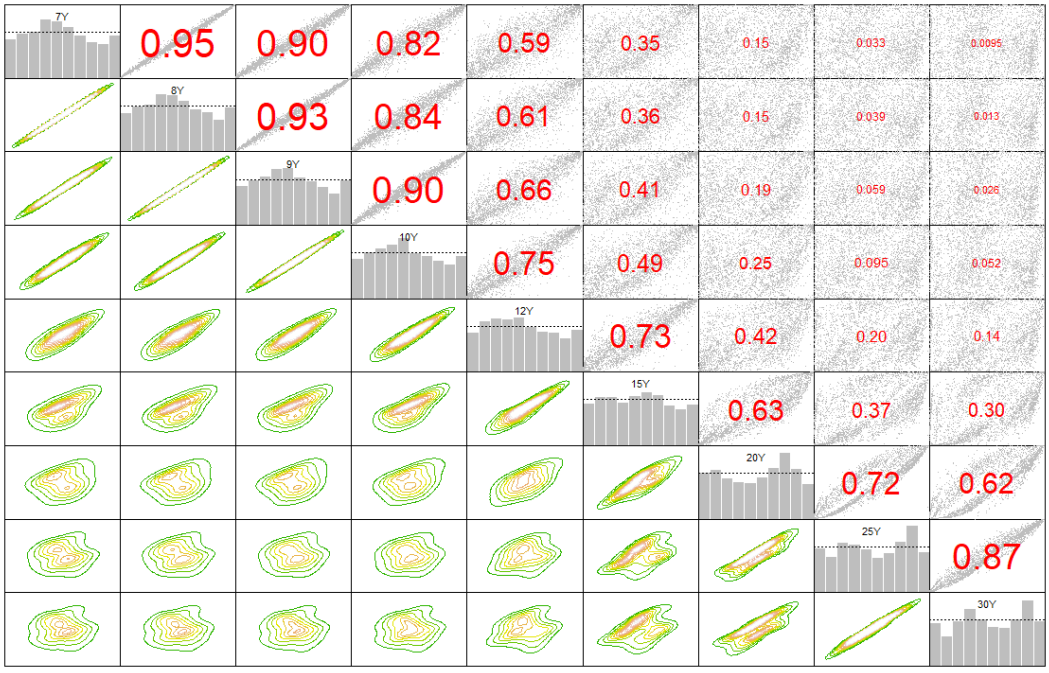

Figure 7: This figure illustrates the pairwise plot of uniform marginals for the yield curve for Germany. The uniform marginals are obtained based on probability transformation (univariate Kernel density) of standardized residuals from the dynamic Nelson-Siegel model in Eqs. (7)-(8). The sample includes daily governmental zero-coupon bond yields, with maturities of one month (1M) to thirty years (30Y), from January 31, 2014, until July 5, 2024.

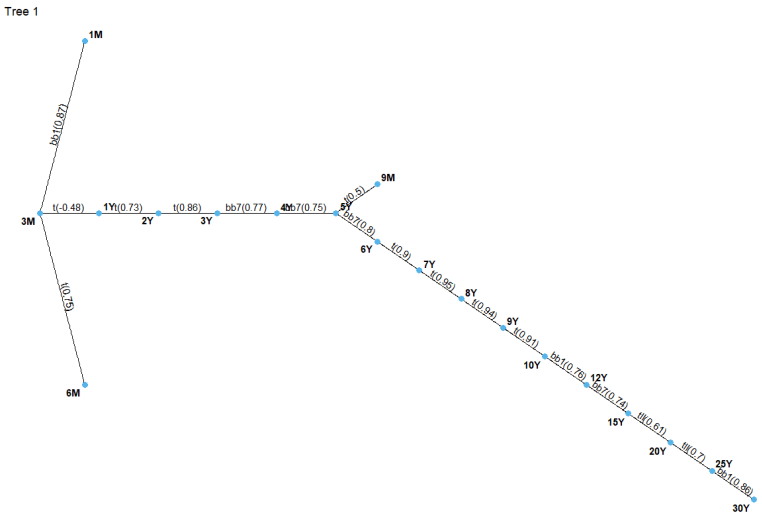

Figure 8: This figure illustrates the first tree, with copula families and Kendall's tau in parentheses, in the truncated Rvine copula structure estimated based on maximum likelihood in Eqs. (4)-(6). The sample includes daily governmental zero-coupon bond yields, with maturities of one month (1M) to thirty years (30Y), from January 31, 2014, until July 5, 2024.

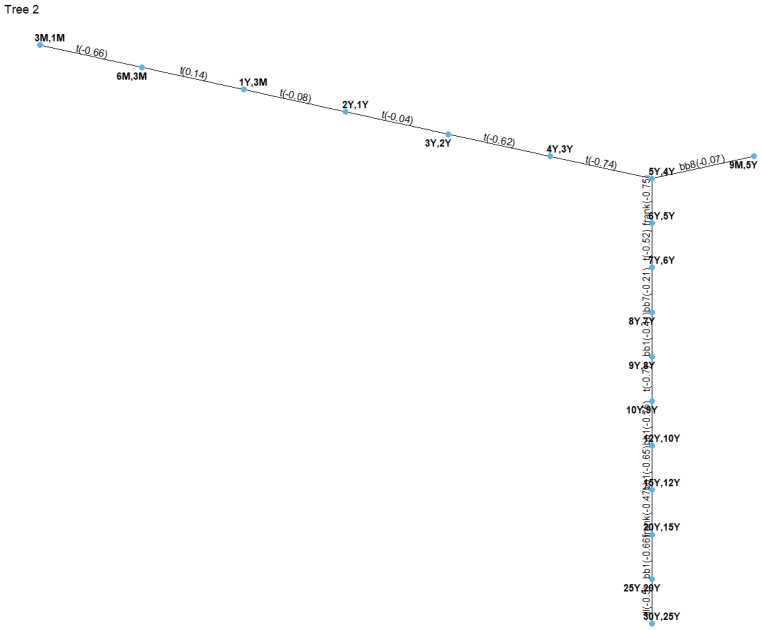

Figure 9: This figure illustrates the second tree, with copula families and Kendall's tau in parentheses, in the truncated Rvine copula structure estimated based on maximum likelihood in Eqs. (4)-(6). The sample includes daily governmental zero-coupon bond yields, with maturities of one month (1M) to thirty years (30Y), from January 31, 2014, until July 5, 2024.

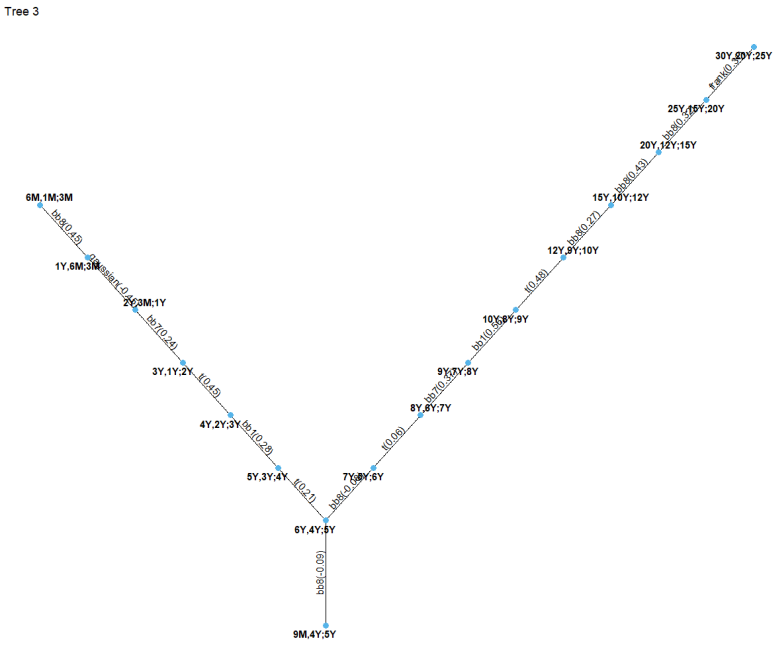

Figure 10: This figure illustrates the third tree, with copula families and Kendall's tau in parentheses, in the truncated Rvine copula structure estimated based on maximum likelihood in Eqs. (4)-(6). The sample includes daily governmental zero-coupon bond yields, with maturities of one month (1M) to thirty years (30Y), from January 31, 2014, until July 5, 2024.

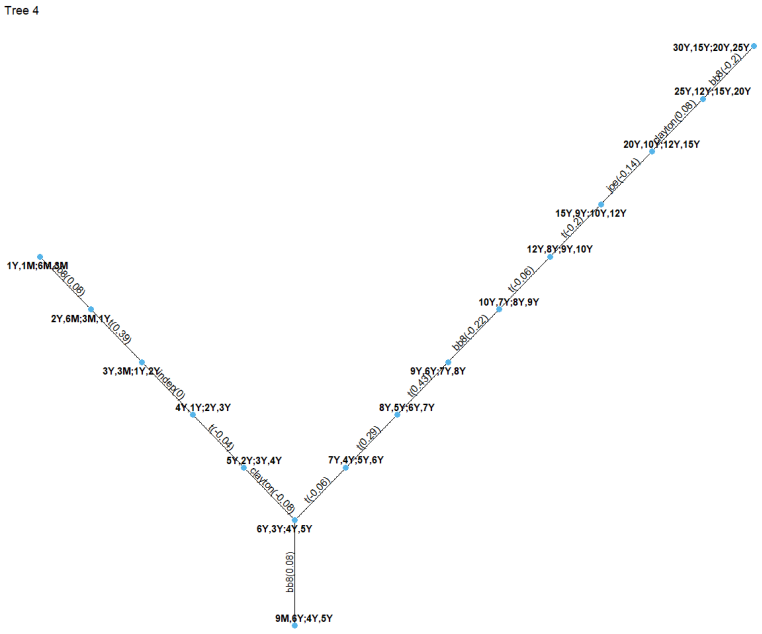

Figure 11: This figure illustrates the fourth tree, with copula families and Kendall's tau in parentheses, in the truncated Rvine copula structure estimated based on maximum likelihood in Eqs. (4)-(6). The sample includes daily governmental zero-coupon bond yields, with maturities of one month (1M) to thirty years (30Y), from January 31, 2014, until July 5, 2024.

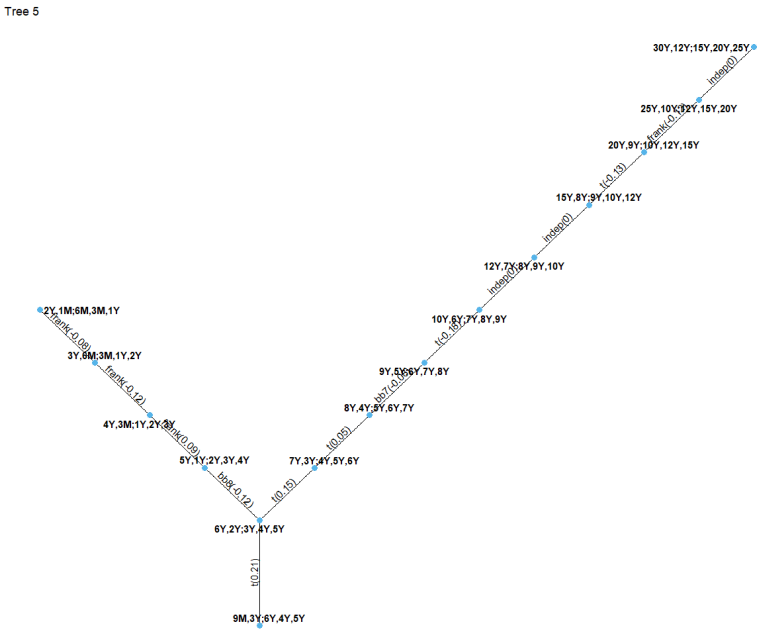

Figure 12: This figure illustrates the fifth tree, with copula families and Kendall's tau in parentheses, in the truncated Rvine copula structure estimated based on maximum likelihood in Eqs. (4)-(6). The sample includes daily governmental zero-coupon bond yields, with maturities of one month (1M) to thirty years (30Y), from January 31, 2014, until July 5, 2024.

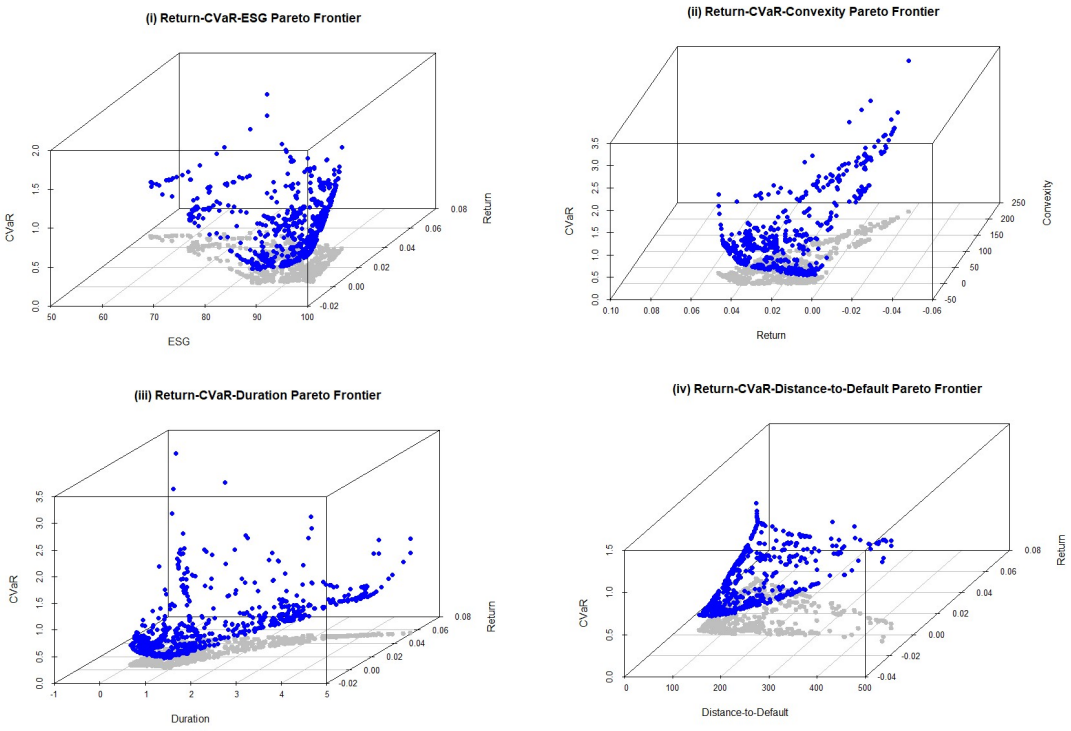

Figure 13: The three-criteria Pareto frontiers obtained by changing investor preference parameters λ by 1% in the MOBP optimization with long-only constraint (see Eq. (20)). The sample includes observed daily total returns, issuer ESG scores, estimated (option-adjusted) duration, (option-adjusted) convexity, as well as distance-to-default for 365 ESG bonds with available returns over the past 500 days up to and including July 5, 2024.

Table 1: Out-of-sample multiobjective ESG-bond Portfolio Performance

	Av. Return (%)	Std. Deviation	CVaR	SR	STARR	ESG	Duration	Convexity	DtD	Min W (%)	Max W (%)	Turnover	Wealth
Panel A: Benchmarks													
EQW	0.862	3.471	0.869	0.248	0.004	75.7	3.852	-36.832	42.879	1.3	1.3	0.022	107.381
Panel A.1: Dynamic Nelson-Siegel Bond Portfolios													
$\lambda_{\Lambda_\mu} = \lambda_{\psi_\zeta} = 1/2$	-0.084	3.214	0.819	-0.026	0.000	76.136	3.686	-35.879	42.73	0.309	4.941	0.223	98.8
$\lambda_{\Lambda_\mu} = \lambda_{\psi_\zeta} = \lambda_{\psi_\mathcal{D}} = 1/3$	0.654	2.552	0.596	0.256	0.004	76.19	2.474	-49.657	43.344	0.309	4.941	0.216	105.674
$\lambda_{\Lambda_\mu} = \lambda_{\psi_\zeta} = \lambda_{\psi_\mathcal{D}} = \lambda_{\Lambda_\mathcal{C}} = 1/4$	0.154	3.127	0.804	0.049	0.001	75.979	4.079	13.583	41.286	0.309	4.941	0.252	100.94
$\lambda_{\Lambda_\mu} = \lambda_{\psi_\zeta} = \lambda_{\psi_\mathcal{D}} = \lambda_{\Lambda_\mathcal{C}} = \lambda_{\Lambda_{\text{DtD}}} = 1/5$	0.354	3.13	0.801	0.113	0.002	75.905	4.101	13.499	44.921	0.309	4.941	0.244	102.748
Panel A.2: Socially Responsible Dynamic Nelson-Siegel Bond Portfolios													
$\lambda_{\Lambda_\mu} = \lambda_{\psi_\zeta} = \lambda_{\Lambda_\theta} = 1/3$	0.178	3.086	0.774	0.058	0.001	79.939	3.617	-31.162	42.031	0.309	4.941	0.251	101.167
$\lambda_{\Lambda_\mu} = \lambda_{\psi_\zeta} = \lambda_{\Lambda_\theta} = \lambda_{\psi_\mathcal{D}} = 1/4$	0.608	2.523	0.599	0.241	0.004	78.027	2.459	-49.058	43.177	0.309	4.941	0.21	105.252
$\lambda_{\Lambda_\mu} = \lambda_{\psi_\zeta} = \lambda_{\Lambda_\theta} = \lambda_{\psi_\mathcal{D}} = \lambda_{\Lambda_\mathcal{C}} = 1/5$	0.183	3.135	0.812	0.058	0.001	77.737	4.097	13.685	41.043	0.309	4.941	0.251	101.193
$\lambda_{\Lambda_\mu} = \lambda_{\psi_\zeta} = \lambda_{\Lambda_\theta} = \lambda_{\psi_\mathcal{D}} = \lambda_{\Lambda_\mathcal{C}} = \lambda_{\Lambda_{\text{DtD}}} = 1/6$	0.262	3.129	0.807	0.084	0.001	77.347	4.099	13.431	44.77	0.309	4.941	0.245	101.906
$\lambda_{\Lambda_\mu} = \lambda_{\psi_\zeta} = \lambda_{\Lambda_\theta} = \lambda_{\psi_\mathcal{D}} = \lambda_{\Lambda_\mathcal{C}} = \lambda_{\Lambda_{\text{DtD}}} = \lambda_{\psi_\vartheta} = 1/7$	0.844	2.746	0.677	0.307	0.005	77.883	3.855	10.591	45.078	0.309	4.941	0.048	107.428
Panel B: Copula-based dynamic Nelson-Siegel Bond Portfolios													
$\lambda_{\Lambda_\mu} = \lambda_{\psi_\zeta} = 1/2$	0.826	2.005	0.419	0.412	0.008	76.83	2.856	-15.189	40.565	0.325	5.45	0.158	107.423
$\lambda_{\Lambda_\mu} = \lambda_{\psi_\zeta} = \lambda_{\psi_\mathcal{D}} = 1/3$	0.972	1.944	0.398	0.5	0.01	76.739	2.517	-21.872	41.158	0.325	5.468	0.158	108.837
$\lambda_{\Lambda_\mu} = \lambda_{\psi_\zeta} = \lambda_{\psi_\mathcal{D}} = \lambda_{\Lambda_\mathcal{C}} = 1/4$	1.303	2.419	0.511	0.539	0.01	76.518	3.761	10.142	40.12	0.324	5.484	0.234	111.981
$\lambda_{\Lambda_\mu} = \lambda_{\psi_\zeta} = \lambda_{\psi_\mathcal{D}} = \lambda_{\Lambda_\mathcal{C}} = \lambda_{\Lambda_{\text{DtD}}} = 1/5$	1.016	2.343	0.504	0.433	0.008	76.346	3.611	8.144	42.43	0.325	5.488	0.21	109.176
Panel C: Socially Responsible Copula-based dynamic Nelson-Siegel Bond Portfolios													
$\lambda_{\Lambda_\mu} = \lambda_{\psi_\zeta} = \lambda_{\Lambda_\theta} = 1/3$	0.824	2.01	0.422	0.41	0.008	77.685	2.842	-15.478	40.483	0.325	5.452	0.158	107.398
$\lambda_{\Lambda_\mu} = \lambda_{\psi_\zeta} = \lambda_{\Lambda_\theta} = \lambda_{\psi_\mathcal{D}} = 1/4$	0.897	1.937	0.395	0.463	0.009	77.469	2.516	-21.474	41.125	0.325	5.455	0.152	108.113
$\lambda_{\Lambda_\mu} = \lambda_{\psi_\zeta} = \lambda_{\Lambda_\theta} = \lambda_{\psi_\mathcal{D}} = \lambda_{\Lambda_\mathcal{C}} = 1/5$	1.088	2.328	0.498	0.467	0.009	77.358	3.622	8.344	39.776	0.325	5.46	0.213	109.884
$\lambda_{\Lambda_\mu} = \lambda_{\psi_\zeta} = \lambda_{\Lambda_\theta} = \lambda_{\psi_\mathcal{D}} = \lambda_{\Lambda_\mathcal{C}} = \lambda_{\Lambda_{\text{DtD}}} = 1/6$	0.952	2.352	0.503	0.405	0.008	77.122	3.61	8.216	42.367	0.325	5.459	0.209	108.556
$\lambda_{\Lambda_\mu} = \lambda_{\psi_\zeta} = \lambda_{\Lambda_\theta} = \lambda_{\psi_\mathcal{D}} = \lambda_{\Lambda_\mathcal{C}} = \lambda_{\Lambda_{\text{DtD}}} = \lambda_{\psi_\vartheta} = 1/7$	1.409	2.16	0.441	0.653	0.013	77.571	3.499	7.054	43.696	0.324	5.45	0.058	113.104

Notes: λ_{Λ_μ}, λ_{ψ_ζ}, λ_{Λ_θ}, $\lambda_{\psi_\mathcal{D}}$, $\lambda_{\Lambda_\mathcal{C}}$, $\lambda_{\Lambda_{\text{DtD}}}$, λ_{ψ_ϑ} denote the weights for portfolio return, CVaR, ESG, duration, convexity, distance-to-default (DtD), and turnover, respectively. Portfolio returns are obtained using rolling window estimation (with 500 days as the training sample) and portfolio back-testing from January 1, 2016, until July 5, 2024, resulting in 2,221 portfolio out-of-sample net returns using 1 basis point proportional transaction cost. The κ parameter in the MOBP problem is set to 4. CVaR is reported at the 1% level. Average returns, standard deviations, and Sharpe ratios (SR) are annualized. Accumulated portfolio wealth is calculated at the end of out-of-sample assuming an initial investment of €100.

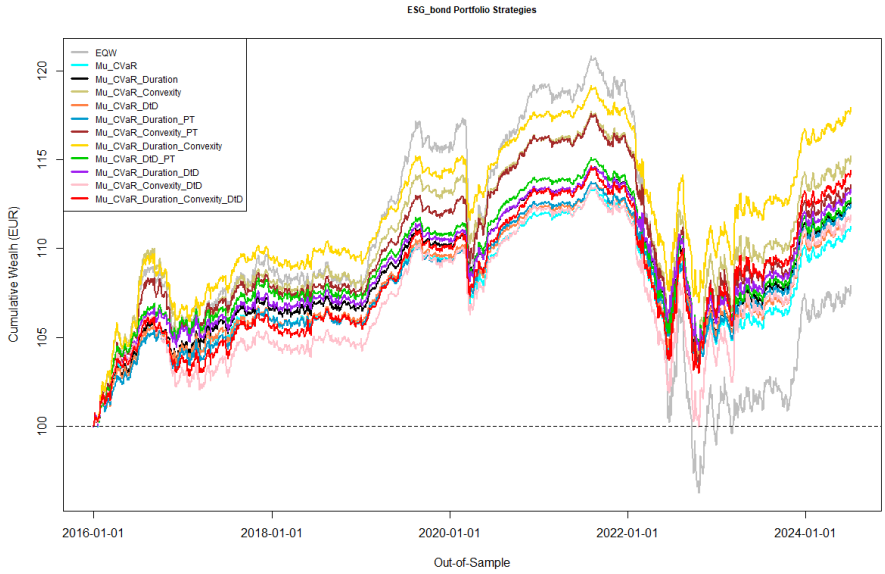

Figure 14: The wealth trajectory for MOBP strategies using the rolling window estimation (with 500 days as the training sample) and portfolio back-testing from January 1, 2016, until July 5, 2024, with an initial investment of €100.

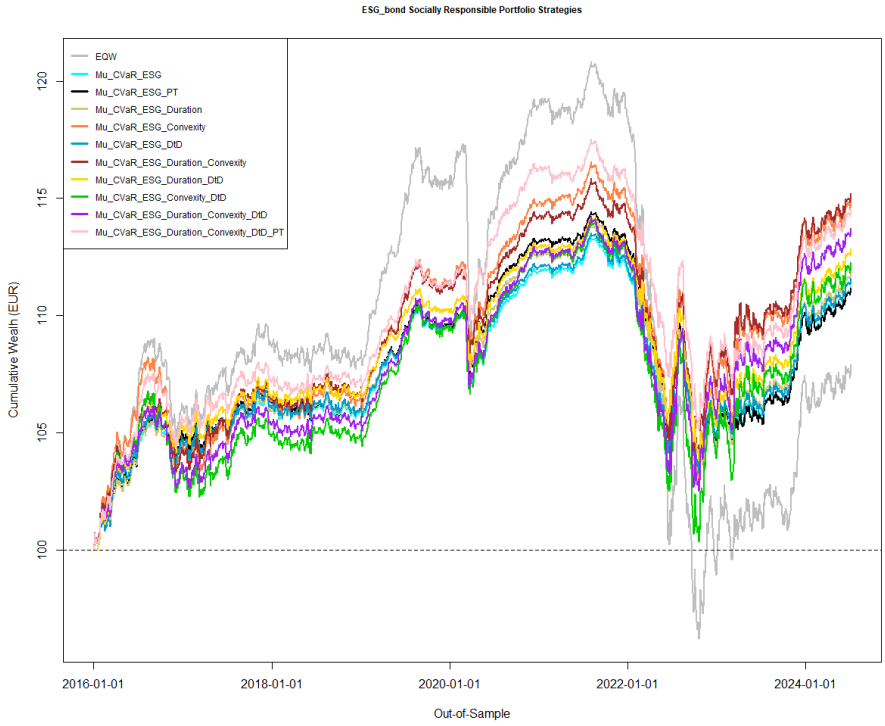

Figure 15: The wealth trajectory for socially responsible MOBP strategies using the rolling window estimation (with 500 days as the training sample) and portfolio back-testing from January 1, 2016, until July 5, 2024, with an initial investment of €100.

Table 2: Robustness Check: $\kappa = 2$

	Av. Return (%)	Std. Deviation	CVaR	SR	STARR	ESG	Duration	Convexity	DtD	Min W (%)	Max W (%)	Turnover	Wealth
Panel A: Benchmarks													
EQW	0.862	3.471	0.869	0.248	0.004	75.7	3.852	-36.832	42.879	1.3	1.3	0.022	107.381
Panel A.1: Dynamic Nelson-Siegel Bond Portfolios													
$\lambda_{\Lambda_\mu} = \lambda_{\psi_\zeta} = 1/2$	0.464	3.128	0.79	0.148	0.002	75.848	3.689	-33.642	42.384	0.618	2.471	0.112	103.756
$\lambda_{\Lambda_\mu} = \lambda_{\psi_\zeta} = \lambda_{\psi_\mathcal{D}} = 1/3$	0.649	2.914	0.725	0.223	0.004	75.867	3.239	-40.298	42.488	0.618	2.471	0.11	105.539
$\lambda_{\Lambda_\mu} = \lambda_{\psi_\zeta} = \lambda_{\psi_\mathcal{D}} = \lambda_{\Lambda_\mathcal{C}} = 1/4$	1.106	3.121	0.789	0.354	0.006	75.855	4.492	2.27	41.25	0.472	2.556	0.064	109.851
$\lambda_{\Lambda_\mu} = \lambda_{\psi_\zeta} = \lambda_{\psi_\mathcal{D}} = \lambda_{\Lambda_\mathcal{C}} = \lambda_{\Lambda_{\text{DtD}}} = 1/5$	1.089	3.127	0.791	0.348	0.006	75.809	4.5	2.371	41.983	0.472	2.556	0.063	109.685
Panel A.2: Socially Responsible Dynamic Nelson-Siegel Bond Portfolios													
$\lambda_{\Lambda_\mu} = \lambda_{\psi_\zeta} = \lambda_{\Lambda_\theta} = 1/3$	0.508	3.132	0.788	0.162	0.003	76.941	3.696	-32.725	42.307	0.618	2.471	0.118	104.162
$\lambda_{\Lambda_\mu} = \lambda_{\psi_\zeta} = \lambda_{\Lambda_\theta} = \lambda_{\psi_\mathcal{D}} = 1/4$	0.663	2.915	0.727	0.228	0.004	76.58	3.236	-40.251	42.457	0.618	2.471	0.11	105.67
$\lambda_{\Lambda_\mu} = \lambda_{\psi_\zeta} = \lambda_{\Lambda_\theta} = \lambda_{\psi_\mathcal{D}} = \lambda_{\Lambda_\mathcal{C}} = 1/5$	1.112	3.12	0.789	0.356	0.006	76.253	4.497	2.386	41.194	0.472	2.556	0.065	109.902
$\lambda_{\Lambda_\mu} = \lambda_{\psi_\zeta} = \lambda_{\Lambda_\theta} = \lambda_{\psi_\mathcal{D}} = \lambda_{\Lambda_\mathcal{C}} = \lambda_{\Lambda_{\text{DtD}}} = 1/6$	1.126	3.128	0.79	0.36	0.006	76.171	4.506	2.432	41.99	0.472	2.556	0.063	110.037
$\lambda_{\Lambda_\mu} = \lambda_{\psi_\zeta} = \lambda_{\Lambda_\theta} = \lambda_{\psi_\mathcal{D}} = \lambda_{\Lambda_\mathcal{C}} = \lambda_{\Lambda_{\text{DtD}}} = \lambda_{\psi_\vartheta} = 1/7$	1.22	3.055	0.776	0.399	0.006	76.368	4.421	0.872	42.337	0.472	2.556	0.018	110.984
Panel B: Copula-based dynamic Nelson-Siegel Bond Portfolios													
$\lambda_{\Lambda_\mu} = \lambda_{\psi_\zeta} = 1/2$	1.345	2.545	0.536	0.528	0.01	76.266	3.353	-22.636	41.422	0.649	2.838	0.097	112.366
$\lambda_{\Lambda_\mu} = \lambda_{\psi_\zeta} = \lambda_{\psi_\mathcal{D}} = 1/3$	1.363	2.504	0.519	0.544	0.011	76.237	3.086	-28.664	41.779	0.649	2.891	0.1	112.563
$\lambda_{\Lambda_\mu} = \lambda_{\psi_\zeta} = \lambda_{\psi_\mathcal{D}} = \lambda_{\Lambda_\mathcal{C}} = 1/4$	1.619	2.897	0.593	0.559	0.011	76.07	4.488	1.548	41.185	0.47	3.869	0.092	115.042
$\lambda_{\Lambda_\mu} = \lambda_{\psi_\zeta} = \lambda_{\psi_\mathcal{D}} = \lambda_{\Lambda_\mathcal{C}} = \lambda_{\Lambda_{\text{DtD}}} = 1/5$	1.648	2.893	0.596	0.57	0.011	76.058	4.471	1.274	42.176	0.47	3.838	0.081	115.341
Panel C: Socially Responsible Copula-based dynamic Nelson-Siegel Bond Portfolios													
$\lambda_{\Lambda_\mu} = \lambda_{\psi_\zeta} = \lambda_{\Lambda_\theta} = 1/3$	1.334	2.543	0.536	0.524	0.01	76.84	3.352	-22.496	41.396	0.649	2.872	0.097	112.258
$\lambda_{\Lambda_\mu} = \lambda_{\psi_\zeta} = \lambda_{\Lambda_\theta} = \lambda_{\psi_\mathcal{D}} = 1/4$	1.33	2.503	0.519	0.531	0.01	76.694	3.088	-28.455	41.775	0.649	2.877	0.095	112.234
$\lambda_{\Lambda_\mu} = \lambda_{\psi_\zeta} = \lambda_{\Lambda_\theta} = \lambda_{\psi_\mathcal{D}} = \lambda_{\Lambda_\mathcal{C}} = 1/5$	1.63	2.886	0.591	0.565	0.011	76.532	4.473	1.451	41.08	0.47	3.867	0.088	115.153
$\lambda_{\Lambda_\mu} = \lambda_{\psi_\zeta} = \lambda_{\Lambda_\theta} = \lambda_{\psi_\mathcal{D}} = \lambda_{\Lambda_\mathcal{C}} = \lambda_{\Lambda_{\text{DtD}}} = 1/6$	1.629	2.892	0.595	0.563	0.011	76.434	4.473	1.418	42.167	0.47	3.832	0.081	115.146
$\lambda_{\Lambda_\mu} = \lambda_{\psi_\zeta} = \lambda_{\Lambda_\theta} = \lambda_{\psi_\mathcal{D}} = \lambda_{\Lambda_\mathcal{C}} = \lambda_{\Lambda_{\text{DtD}}} = \lambda_{\psi_\vartheta} = 1/7$	1.786	2.81	0.574	0.636	0.012	76.838	4.384	0.228	42.557	0.47	3.866	0.038	116.787

Notes: λ_{Λ_μ}, λ_{ψ_ζ}, λ_{Λ_θ}, $\lambda_{\psi_\mathcal{D}}$, $\lambda_{\Lambda_\mathcal{C}}$, $\lambda_{\Lambda_{\text{DtD}}}$, λ_{ψ_ϑ} denote the weights for portfolio return, CVaR, ESG, duration, convexity, distance-to-default (DtD), and turnover, respectively. Portfolio returns are obtained using rolling window estimation (with 500 days as the training sample) and portfolio back-testing from January 1, 2016, until July 5, 2024, resulting in 2,221 portfolio out-of-sample net returns using 1 basis point proportional transaction cost. The κ parameter in the MOBP problem is set to 2. CVaR is reported at the 1% level. Average returns, standard deviations, and Sharpe ratios (SR) are annualized. Accumulated portfolio wealth is calculated at the end of out-of-sample assuming an initial investment of €100.

Table 3: Robustness Check: $\kappa = 10$

	Av. Return (%)	Std. Deviation	CVaR	SR	STARR	ESG	Duration	Convexity	DtD	Min W (%)	Max W (%)	Turnover	Wealth
Panel A: Benchmarks													
EQW	0.862	3.471	0.869	0.248	0.004	75.7	3.852	-36.832	42.879	1.3	1.3	0.022	107.381
Panel A.1: Dynamic Nelson-Siegel Bond Portfolios													
$\lambda_{\Lambda_\mu} = \lambda_{\psi_\zeta} = 1/2$	-0.186	3.812	0.939	-0.049	-0.001	76.379	3.937	-47.392	43.353	0.124	12.353	0.365	97.726
$\lambda_{\Lambda_\mu} = \lambda_{\psi_\zeta} = \lambda_{\psi_\mathcal{D}} = 1/3$	0.865	1.991	0.486	0.434	0.007	77.18	1.343	-48.651	44.119	0.124	12.353	0.307	107.796
$\lambda_{\Lambda_\mu} = \lambda_{\psi_\zeta} = \lambda_{\psi_\mathcal{D}} = \lambda_{\Lambda_\mathcal{C}} = 1/4$	-0.318	3.345	0.842	-0.095	-0.002	76.106	3.553	21.471	42.163	0.124	12.353	0.488	96.736
$\lambda_{\Lambda_\mu} = \lambda_{\psi_\zeta} = \lambda_{\psi_\mathcal{D}} = \lambda_{\Lambda_\mathcal{C}} = \lambda_{\Lambda_{\text{DtD}}} = 1/5$	-0.655	3.278	0.827	-0.2	-0.003	76.43	3.608	20.279	50.976	0.124	12.352	0.453	93.899
Panel A.2: Socially Responsible Dynamic Nelson-Siegel Bond Portfolios													
$\lambda_{\Lambda_\mu} = \lambda_{\psi_\zeta} = \lambda_{\Lambda_\theta} = 1/3$	-0.18	3.422	0.828	-0.053	-0.001	85.45	3.721	-31.01	41.434	0.124	12.353	0.353	97.903
$\lambda_{\Lambda_\mu} = \lambda_{\psi_\zeta} = \lambda_{\Lambda_\theta} = \lambda_{\psi_\mathcal{D}} = 1/4$	1.131	2.000	0.475	0.566	0.010	81.027	1.409	-49.233	44.530	0.124	12.353	0.297	110.376
$\lambda_{\Lambda_\mu} = \lambda_{\psi_\zeta} = \lambda_{\Lambda_\theta} = \lambda_{\psi_\mathcal{D}} = \lambda_{\Lambda_\mathcal{C}} = 1/5$	-0.56	3.315	0.858	-0.169	-0.003	80.473	3.531	20.819	41.426	0.124	12.353	0.47	94.68
$\lambda_{\Lambda_\mu} = \lambda_{\psi_\zeta} = \lambda_{\Lambda_\theta} = \lambda_{\psi_\mathcal{D}} = \lambda_{\Lambda_\mathcal{C}} = \lambda_{\Lambda_{\text{DtD}}} = 1/6$	-0.31	3.257	0.835	-0.095	-0.001	79.242	3.585	19.827	50.723	0.124	12.352	0.447	96.827
$\lambda_{\Lambda_\mu} = \lambda_{\psi_\zeta} = \lambda_{\Lambda_\theta} = \lambda_{\psi_\mathcal{D}} = \lambda_{\Lambda_\mathcal{C}} = \lambda_{\Lambda_{\text{DtD}}} = \lambda_{\psi_\vartheta} = 1/7$	0.644	2.603	0.631	0.248	0.004	79.715	3.285	16.82	50.497	0.124	12.166	0.082	105.574
Panel B: Copula-based dynamic Nelson-Siegel Bond Portfolios													
$\lambda_{\Lambda_\mu} = \lambda_{\psi_\zeta} = 1/2$	0.916	1.735	0.347	0.528	0.011	77.374	2.44	-9.82	40.333	0.129	13.193	0.29	108.333
$\lambda_{\Lambda_\mu} = \lambda_{\psi_\zeta} = \lambda_{\psi_\mathcal{D}} = 1/3$	0.824	1.566	0.348	0.526	0.009	77.189	1.542	-31.226	42.339	0.129	13.192	0.257	107.477
$\lambda_{\Lambda_\mu} = \lambda_{\psi_\zeta} = \lambda_{\psi_\mathcal{D}} = \lambda_{\Lambda_\mathcal{C}} = 1/4$	0.393	1.677	0.38	0.234	0.004	77.066	2.367	6.966	40.237	0.129	13.212	0.331	103.423
$\lambda_{\Lambda_\mu} = \lambda_{\psi_\zeta} = \lambda_{\psi_\mathcal{D}} = \lambda_{\Lambda_\mathcal{C}} = \lambda_{\Lambda_{\text{DtD}}} = 1/5$	0.713	1.742	0.389	0.41	0.007	76.963	2.418	7.514	44.836	0.129	13.164	0.291	106.399
Panel C: Socially Responsible Copula-based dynamic Nelson-Siegel Bond Portfolios													
$\lambda_{\Lambda_\mu} = \lambda_{\psi_\zeta} = \lambda_{\Lambda_\theta} = 1/3$	0.522	1.649	0.344	0.317	0.006	79.06	2.322	-13.235	39.84	0.13	13.248	0.282	104.625
$\lambda_{\Lambda_\mu} = \lambda_{\psi_\zeta} = \lambda_{\Lambda_\theta} = \lambda_{\psi_\mathcal{D}} = 1/4$	0.806	1.556	0.323	0.518	0.01	78.933	1.621	-27.766	41.682	0.129	13.158	0.231	107.308
$\lambda_{\Lambda_\mu} = \lambda_{\psi_\zeta} = \lambda_{\Lambda_\theta} = \lambda_{\psi_\mathcal{D}} = \lambda_{\Lambda_\mathcal{C}} = 1/5$	0.786	1.646	0.357	0.478	0.009	79	2.369	6.695	39.672	0.129	13.201	0.267	107.106
$\lambda_{\Lambda_\mu} = \lambda_{\psi_\zeta} = \lambda_{\Lambda_\theta} = \lambda_{\psi_\mathcal{D}} = \lambda_{\Lambda_\mathcal{C}} = \lambda_{\Lambda_{\text{DtD}}} = 1/6$	0.945	1.735	0.381	0.544	0.01	78.573	2.407	7.384	44.837	0.129	13.166	0.27	108.61
$\lambda_{\Lambda_\mu} = \lambda_{\psi_\zeta} = \lambda_{\Lambda_\theta} = \lambda_{\psi_\mathcal{D}} = \lambda_{\Lambda_\mathcal{C}} = \lambda_{\Lambda_{\text{DtD}}} = \lambda_{\psi_\vartheta} = 1/7$	1.287	1.792	0.381	0.718	0.014	78.97	2.519	8.546	45.403	0.129	12.915	0.082	111.951

Notes: λ_{Λ_μ}, λ_{ψ_ζ}, λ_{Λ_θ}, $\lambda_{\psi_\mathcal{D}}$, $\lambda_{\Lambda_\mathcal{C}}$, $\lambda_{\Lambda_{\text{DtD}}}$, λ_{ψ_ϑ} denote the weights for portfolio return, CVaR, ESG, duration, convexity, distance-to-default (DtD), and turnover, respectively. Portfolio returns are obtained using rolling window estimation (with 500 days as the training sample) and portfolio back-testing from January 1, 2016, until July 5, 2024, resulting in 2,221 portfolio out-of-sample net returns using 1 basis point proportional transaction cost. The κ parameter in the MOBP problem is set to 10. CVaR is reported at the 1% level. Average returns, standard deviations, and Sharpe ratios (SR) are annualized. Accumulated portfolio wealth is calculated at the end of out-of-sample assuming an initial investment of €100.

Table 4: Robustness Check: CO2 Emissions

	Av. Return (%)	Std. Deviation	CVaR	SR	STARR	CO2	Duration	Convexity	DtD	Min W (%)	Max W (%)	Turnover	Wealth
Panel A: Benchmarks													
EQW	0.862	3.471	0.869	0.248	0.004	10763533	3.852	-36.832	42.879	1.3	1.3	0.022	107.381
Panel B: MOBPs with CO2 Emission													
$\lambda_{\Lambda_\mu} = \lambda_{\psi_\zeta} = \lambda_{\Lambda_{\text{CO2}}} = 1/3$	1.193	2.624	0.596	0.455	0.008	4196836	3.193	-15.948	40.279	0.305	7.354	0.106	110.839
$\lambda_{\Lambda_\mu} = \lambda_{\psi_\zeta} = \lambda_{\Lambda_{\text{CO2}}} = \lambda_{\psi_\mathcal{D}} = 1/4$	1.533	2.739	0.609	0.56	0.01	4612932	2.921	-24.244	41.284	0.308	7.965	0.11	114.214
$\lambda_{\Lambda_\mu} = \lambda_{\psi_\zeta} = \lambda_{\Lambda_{\text{CO2}}} = \lambda_{\psi_\mathcal{D}} = \lambda_{\Lambda_\mathcal{C}} = 1/5$	1.169	3.339	0.766	0.35	0.006	3777236	4.407	15.345	38.627	0.305	7.839	0.114	110.398
$\lambda_{\Lambda_\mu} = \lambda_{\psi_\zeta} = \lambda_{\Lambda_{\text{CO2}}} = \lambda_{\psi_\mathcal{D}} = \lambda_{\Lambda_\mathcal{C}} = \lambda_{\Lambda_{\text{DtD}}} = 1/6$	1.317	2.993	0.679	0.44	0.008	3843572	4.223	13.161	40.543	0.304	6.955	0.118	111.963
$\lambda_{\Lambda_\mu} = \lambda_{\psi_\zeta} = \lambda_{\Lambda_{\text{CO2}}} = \lambda_{\psi_\mathcal{D}} = \lambda_{\Lambda_\mathcal{C}} = \lambda_{\Lambda_{\text{DtD}}} = \lambda_{\psi_\partial} = 1/7$	1.38	3.024	0.681	0.456	0.008	3189056	4.312	12.887	41.649	0.268	7.308	0.044	112.589

Notes: λ_{Λ_μ}, λ_{ψ_ζ}, $\lambda_{\Lambda_{\text{CO2}}}$, $\lambda_{\psi_\mathcal{D}}$, $\lambda_{\Lambda_\mathcal{C}}$, $\lambda_{\Lambda_{\text{DtD}}}$, λ_{ψ_∂} denote the weights for portfolio return, CVaR, CO2 emission (level), duration, convexity, distance-to-default (DtD), and turnover, respectively. Portfolio returns are obtained using rolling window estimation (with 500 days as the training sample) and portfolio back-testing from January 1, 2016, until July 5, 2024, resulting in 2,221 portfolio out-of-sample net returns using 1 basis point proportional transaction cost. The κ parameter in the MOBP problem is set to 4. CVaR is reported at the 1% level. Average returns, standard deviations, and Sharpe ratios (SR) are annualized. Accumulated portfolio wealth is calculated at the end of out-of-sample assuming an initial investment of €100.

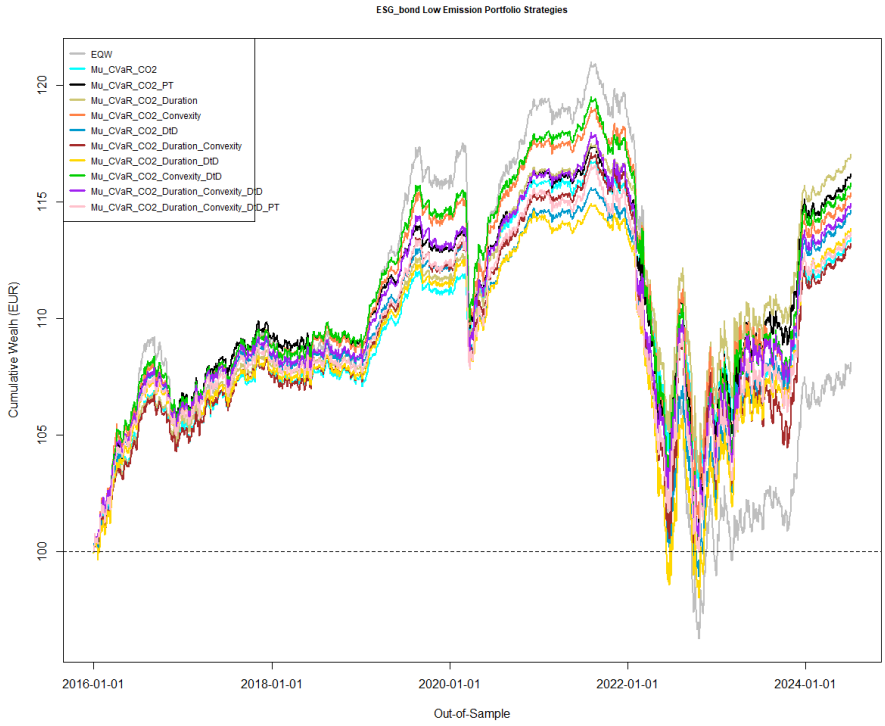

Figure 16: The wealth trajectory for low-emission MOBP strategies using the rolling window estimation (with 500 days as the training sample) and portfolio back-testing from January 1, 2016, until July 5, 2024, with an initial investment of €100.

References

Aas, K., Czado, C., Frigessi, A. and Bakken, H. (2009), 'Pair-copula constructions of multiple dependence', *Insurance: Mathematics and Economics* **44**(2), 182–198.

Acar, E. F., Genest, C. and NešLehová, J. (2012), 'Beyond simplified pair-copula constructions', *Journal of Multivariate Analysis* **110**, 74–90.

Afik, Z., Arad, O. and Galil, K. (2016), 'Using merton model for default prediction: An empirical assessment of selected alternatives', *Journal of Empirical Finance* **35**, 43–67.

Bedford, T. and Cooke, R. M. (2001), 'Probability density decomposition for conditionally dependent random variables modeled by vines', *Annals of Mathematics and Artificial Intelligence* **32**(1-4), 245–268.

Bedford, T. and Cooke, R. M. (2002), 'Vines - A new graphical model for dependent random variables', *Annals of Statistics* **30**(4), 1031–1068.

Bharath, S. T. and Shumway, T. (2008), 'Forecasting default with the merton distance to default model', *The Review of Financial Studies* **21**(3), 1339–1369.

Black, F. and Cox, J. C. (1976), 'Valuing corporate securities: Some effects of bond indenture provisions', *The Journal of Finance* **31**(2), 351–367.

Bradley, S. P. and Crane, D. B. (1972), 'A dynamic model for bond portfolio management', *Management Science* **19**(2), 139–151.

Brechmann, E. C., Czado, C. and Aas, K. (2012), 'Truncated regular vines in high dimensions with application to financial data', *Canadian Journal of Statistics* **40**(1), 68–85.

Brechmann, E. C. and Joe, H. (2015), 'Truncation of vine copulas using fit indices', *Journal of Multivariate Analysis* **138**, 19–33.

Byrne, J. P., Cao, S. and Korobilis, D. (2017), 'Forecasting the term structure of government bond yields in unstable environments', *Journal of Empirical Finance* **44**, 209–225.

Caldeira, J. F., Moura, G. V. and Santos, A. A. (2016), 'Bond portfolio optimization using dynamic factor models', *Journal of Empirical Finance* **37**, 128–158.

Caldeira, J. F., Moura, G. V. and Santos, A. A. (2018), 'Yield curve forecast combinations based on bond portfolio performance', *Journal of Forecasting* **37**(1), 64–82.

Cao, Y., Fuentes-Cortes, L. F., Chen, S. and Zavala, V. M. (2017), 'Scalable modeling and solution of stochastic multiobjective optimization problems', *Computers & Chemical Engineering* **99**, 185–197.

CBI (2023), 'Sustainable debt: Global state of the market 2023'.
URL: *https://www.climatebonds.net/files/reports/cbi_sotm23_02h.pdf*

Cheng, P. L. (1962), 'Optimum bond portfolio selections', *Management Science* **8**(4), 490–499.

Christensen, J. H., Diebold, F. X. and Rudebusch, G. D. (2009), 'An arbitrage-free generalized nelson—siegel term structure model', *Econometrics Journal* **12**, C33–C64.

Christensen, J. H., Diebold, F. X. and Rudebusch, G. D. (2011), 'The affine arbitrage-free class of nelson–siegel term structure models', *Journal of Econometrics* **164**(1), 4–20.

Cox, J. C., Ingersoll Jr, J. E. and Ross, S. A. (1985), 'A theory of the term structure of interest rates', *Econometrica* **53**(2), 385–407.

Crouhy, M., Galai, D. and Mark, R. (2000), 'A comparative analysis of current credit risk models', *Journal of Banking & Finance* **24**(1-2), 59–117.

Czado, C. (2019), *Analyzing Dependent Data with Vine Copulas. A Practical Guide With R*, Lecture Notes in Statistics, Springer, Cham.

Dai, Q. and Singleton, K. J. (2000), 'Specification analysis of affine term structure models', *The Journal of Finance* **55**(5), 1943–1978.

Deguest, R., Fabozzi, F., Martellini, L. and Milhau, V. (2018), 'Bond portfolio optimization in the presence of duration constraints', *The Journal of Fixed Income* **28**(1), 6–26.

DeMiguel, V., Garlappi, L. and Uppal, R. (2009), 'Optimal versus naive diversification: How inefficient is the 1/n portfolio strategy?', *The Review of Financial Studies* **22**(5), 1915–1953.

Diebold, F. X. and Li, C. (2006), 'Forecasting the term structure of government bond yields', *Journal of Econometrics* **130**(2), 337–364.

Diebold, F. X., Rudebusch, G. D. and Aruoba, S. B. (2006), 'The macroeconomy and the yield curve: a dynamic latent factor approach', *Journal of Econometrics* **131**(1-2), 309–338.

Duffee, G. R. (2002), 'Term premia and interest rate forecasts in affine models', *The Journal of Finance* **57**(1), 405–443.

Duffie, D. and Kan, R. (1996), 'A yield-factor model of interest rates', *Mathematical Finance* **6**(4), 379–406.

Duffie, D., Saita, L. and Wang, K. (2007), 'Multi-period corporate default prediction with stochastic covariates', *Journal of financial economics* **83**(3), 635–665.

Dunetz, M. L. and Mahoney, J. M. (1988), 'Using duration and convexity in the analysis of callable bonds', *Financial Analysts Journal* **44**(3), 53–72.

Fabozzi, F. J. (1999), *Duration, convexity, and other bond risk measures*, Vol. 58, John Wiley & Sons.

GISA (2022), 'Global sustainable investment review 2022'.
URL: *https://www.gsi-alliance.org/wp-content/uploads/2023/12/GSIA-Report-2022.pdf*

Haff, I. H. et al. (2013), 'Parameter estimation for pair-copula constructions', *Bernoulli* **19**(2), 462–491.

Heinen, A., Valdesogo, A. et al. (2009), *Asymmetric CAPM dependence for large dimensions: the canonical vine autoregressive model*, No. Universidad Carlos III de Madrid.

Hodges, S. D. and Schaefer, S. M. (1977), 'A model for bond portfolio improvement', *Journal of Financial and Quantitative Analysis* **12**(2), 243–260.

Hull, J. and White, A. (1990), 'Valuing derivative securities using the explicit finite difference method', *Journal of Financial and Quantitative Analysis* **25**(1), 87–100.

Jagannathan, R. and Ma, T. (2003), 'Risk reduction in large portfolios: Why imposing the wrong constraints helps', *The Journal of Finance* **58**(4), 1651–1683.

Jessen, C. and Lando, D. (2015), 'Robustness of distance-to-default', *Journal of Banking & Finance* **50**, 493–505.

Joe, H. (1996), Families of m-variate distributions with given margins and $m(m-1)/2$ bivariate dependence parameters, *in* M. Ruschendorf, L., Schweizer, B., Taylor, ed., 'Distributions with Fixed Marginals and Related Topics', pp. 120–141.

Joe, H. (2014), *Dependence modeling with copulas*, Chapman & Hall/CRC.

Junker, M., Szimayer, A. and Wagner, N. (2006), 'Nonlinear term structure dependence: Copula functions, empirics, and risk implications', *Journal of Banking & Finance* **30**(4), 1171–1199.

Koopman, S. J., Mallee, M. I. and Van der Wel, M. (2010), 'Analyzing the term structure of interest rates using the dynamic nelson–siegel model with time-varying parameters', *Journal of Business & Economic Statistics* **28**(3), 329–343.

Korn, O. and Koziol, C. (2006), 'Bond portfolio optimization: A risk-return approach', *The Journal of Fixed Income* **15**(4), 48.

Kurowicka, D. (2011), Optimal truncation of vines, *in* D. Kurowicka and H. Joe, eds, 'Dependence Modeling: Vine Copula Handbook', World Scientific Publishing Co.

Levant, J. and Ma, J. (2016), 'Investigating United Kingdom's monetary policy with macro-factor augmented dynamic Nelson–Siegel models', *Journal of Empirical Finance* **37**, 117–127.

Longstaff, F. A. and Schwartz, E. S. (1995), 'A simple approach to valuing risky fixed and floating rate debt', *The Journal of Finance* **50**(3), 789–819.

Markowitz, H. (1952), 'Portfolio selection', *The Journal of Finance* **7**(1), 77–91.

Merton, R. C. (1974), 'On the pricing of corporate debt: The risk structure of interest rates', *The Journal of Finance* **29**(2), 449–470.

Nagler, T. (2024), *kde1d: Univariate Kernel Density Estimation*. R package version 1.0.7.
URL: *https://cran.r-project.org/package=kde1d*

Nagler, T. and Vatter, T. (2021), *rvinecopulib: High Performance Algorithms for Vine Copula Modeling*. R package version 0.5.5.1.1.
URL: *https://cran.r-project.org/package=rvinecopulib*

Nelson, C. R. and Siegel, A. F. (1987), 'Parsimonious modeling of yield curves', *Journal of Business* pp. 473–489.

Rockafellar, R. T. and Uryasev, S. (2000), 'Optimization of conditional Value-at-Risk', *Journal of Risk* **2**, 21–42.

Roll, R. (1971), 'Investment diversification and bond maturity', *The Journal of Finance* **26**(1), 51–66.

Ronn, E. I. (1987), 'A new linear programming approach to bond portfolio management', *Journal of Financial and Quantitative Analysis* **22**(4), 439–466.

Sahamkhadam, M. and Stephan, A. (2024), 'Socially responsible multiobjective optimal portfolios', *Journal of the Operational Research Society* pp. 1–12.

Schaefer, S. M. and Strebulaev, I. A. (2008), 'Structural models of credit risk are useful: Evidence from hedge ratios on corporate bonds', *Journal of Financial Economics* **90**(1), 1–19.

Steuer, R. E., Qi, Y. and Hirschberger, M. (2005), 'Multiple objectives in portfolio selection', *Journal of Financial Decision Making* **1**(1), 5–20.

Steuer, R. E., Qi, Y. and Hirschberger, M. (2007), 'Suitable-portfolio investors, nondominated frontier sensitivity, and the effect of multiple objectives on standard portfolio selection', *Annals of Operations Research* **152**(1), 297–317.

Tu, A. H. and Chen, C. Y.-H. (2018), 'A factor-based approach of bond portfolio value-at-risk: The informational roles of macroeconomic and financial stress factors', *Journal of Empirical Finance* **45**, 243–268.

Vasicek, O. (1977), 'An equilibrium characterization of the term structure', *Journal of financial economics* **5**(2), 177–188.

Vassiadou-Zeniou, C. and Zenios, S. A. (1996), 'Robust optimization models for managing callable bond portfolios', *European Journal of Operational Research* **91**(2), 264–273.

Zenios, S. A. (1995), 'Asset/liability management under uncertainty for fixed-income securities', *Annals of Operations Research* **59**(1), 77–97.

Zumbach, G. (2013), 'A mean/variance approach to long-term fixed-income portfolio allocation', *Quantitative Finance* **13**(9), 1459–1471.